Comparison of modeled versus measured MSA

Gondwe, Mtinkheni; Krol, Maarten; Klaassen, Wim; Gieskes, Winfried; de Baar, Hein

Published in:
Global Biogeochemical Cycles

DOI:
10.1029/2003gb002144

Publication date:
2004

Comparison of modeled versus measured MSA:nss $SO_4^=$ ratios: A global analysis

Mtinkheni Gondwe
Marine Biology Department, University of Groningen, Haren, Netherlands

Maarten Krol
Institute for Marine and Atmospheric Research (IMAU), University of Utrecht, Utrecht, Netherlands

Wim Klaassen, Winfried Gieskes, and Hein de Baar[1]
Marine Biology Department, University of Groningen, Haren, Netherlands

Received 9 September 2003; revised 26 February 2004; accepted 24 March 2004; published 18 May 2004.

[1] The MSA:nss $SO_4^=$ ratio, which is a measure of the relative marine biogenic contribution to the total atmospheric sulphur burden, has long been measured in various parts of the globe. Transect studies and observations from a network of stations have provided some idea of the spatial and temporal behavior of the ratio in various regions, but gaps in knowledge still exist in other parts of the globe. Here we present results of a global 3-D chemical transport modeling study which complement these measurements and provide a globe-wide picture of the spatial variation and distribution of this ratio. Comparison of modeled versus measured data on the MSA:nss $SO_4^=$ ratio resulting from all sulphur sources considered shows fair model performance (i.e., a general overestimation of 23%; degrees of freedom = 90) in all areas of the globe where actual measurements of the ratio have been made. On the other hand, the model-observation comparisons for the MSA:nss $SO_4^=$ ratio derived solely from the oceanic DMS source are not as satisfactory (an overall overestimation of a factor of 3; degrees of freedom = 50). The MSA:nss $SO_4^=$ ratio that is derived from the oceanic DMS source alone provides information on the relative yields of MSA and $SO_4^=$ from atmospheric DMS oxidation. Our model results are consistent with measurements, showing that the ratio is highest around the polar regions and lowest within the tropics. This spatial trend is attributed to the fact that MSA production occurs best under low temperatures (maximum ambient temperature of 27°C). Despite MSA being preferably produced under low temperatures, observations at high latitudes have consistently shown summer maxima and winter minima in the MSA:nss $SO_4^=$ ratio. This has raised many questions on the robustness of the theory of the MSA production mechanism. Diminished marine biological activity and low seawater DMS conditions in winter have widely been cited as the cause of this observed trend. In this study, we further propose that since photochemical hydroxyl radical (OH) production during the dark winter months at polar latitudes is non-existent, reduced wintertime oxidation of DMS by OH to form MSA results in summer maxima and winter minima in MSA concentrations at these latitudes. Temperature and marine biological activity are, therefore, not the only major determining factors for MSA production at high latitudes on a seasonal scale. Light conditions are also important. Throughout the year, the highest ratios occur in the Southern Hemisphere, where the atmospheric DMS burden is highest. This is in agreement with both short- and long-term measurements in literature. *INDEX TERMS:* 1615 Global Change: Biogeochemical processes (4805); 3339 Meteorology and Atmospheric Dynamics: Ocean/atmosphere interactions (0312, 4504); 4801 Oceanography: Biological and Chemical: Aerosols (0305); 4842 Oceanography: Biological and Chemical: Modeling; *KEYWORDS:* global biogeochemical cycles, marine phytoplankton-climate interactions, MSA:nss $SO_4^=$ ratios

[1]Also at Royal Netherlands Institute for Sea Research (KNIOZ), Texel, Netherlands.

0886-6236/04/2003GB002144

Citation: Gondwe, M., M. Krol, W. Klaassen, W. Gieskes, and H. de Baar (2004), Comparison of modeled versus measured MSA:nss $SO_4^=$ ratios: A global analysis, *Global Biogeochem. Cycles*, *18*, GB2006, doi:10.1029/2003GB002144.

1. Introduction

[2] One of the major ecological phenomena on Earth is the occurrence of spatially extensive algal blooms in coastal areas and temperate and polar regions of the global ocean (Figure 1). Besides their role as primary producers, these marine phytoplankton are thought to play an important role in the Earth's energy balance. Some phytoplankton species produce dimethylsulphoniopropionate (DMSP), a precursor compound to the volatile dimethylsulphide (DMS) [*Kiene et al.*, 2000]. Some DMS is emitted into the atmosphere, where it undergoes chemical transformation to eventually form methanesulphonate (MSA) and excess or non sea salt (nss) sulphate aerosols ($SO_4^=$) among other sulphur products [*Charlson et al.*, 1987]. Sulphate aerosols play an important role in the Earth-atmosphere radiation balance through partial scattering, absorption and reflection of solar and terrestrial radiation. They may also serve as nucleation sites for the formation of cloud droplets [*O'Dowd et al.*, 1997] which, in turn, play an important role in the Earth's climate through partial scattering, reflection, and absorption of solar and terrestrial radiation [*Albrecht*, 1989; *Boucher and Lohmann*, 1995].

[3] MSA is formed exclusively from DMS, while nss $SO_4^=$ has a variety of sources which include atmospheric DMS oxidation and volcanic and anthropogenic sulphur emissions. As such, the methanesulphonate to non sea salt sulphate (MSA:nss $SO_4^=$) ratio provides an indication of the relative contributions of DMS and anthropogenic sources to total sulphate levels. A high ratio suggests that a considerable fraction of the total nss $SO_4^=$ burden being observed is derived from the atmospheric oxidation of DMS, while a low ratio implies that the contribution of DMS to the total nss $SO_4^=$ burden being observed is low.

[4] Several isotopic analyses, ice core and atmospheric measurement studies on the MSA:nss $SO_4^=$ ratio have been conducted in the last few decades (e.g., references in Tables 1 and 2) with the purpose of estimating the biogenic fraction of nss $SO_4^=$ over various regions and during different periods (see Figure 2 for location of measurement sites). Several researchers [e.g., *Saltzman et al.*, 1986; *Savoie and Prospero*, 1989; *Savoie et al.*, 2002] have studied the temporal and spatial variability of MSA and nss $SO_4^=$ in aerosols over the Pacific Ocean using long-term measurement records from a network of island based stations, and so trends in the MSA:nss $SO_4^=$ ratio this region of the globe are well documented. Similarly, measurement campaigns along transects [e.g., *Huebert et al.*, 1993; *Pszenny et al.*, 1990] provide data that can be used to determine the latitudinal and longitudinal distribution of the MSA:nss $SO_4^=$ ratio in various regions. However, these data are still not enough to present a comprehensive image of the spatial and temporal behavior of the ratio on a globe-wide scale.

[5] The contribution of ocean-leaving DMS to the total sulphur burden relative to an anthropogenic source can be expected to differ in different areas of the globe and at different times of the year, depending on various reasons such as the location and strength of major sulphur sources and the prevailing atmospheric conditions. In this paper, we use three-dimensional global chemical transport modeling to complement measurements made so far and present a globe-wide picture of the spatial distribution of the MSA:nss $SO_4^=$ ratio. Model results are compared to measurements to assess the model's performance in simulating close-to-observed yields of DMS oxidation products.

2. Data and Methodology

[6] We have conducted three-dimensional atmospheric chemical transport modeling of the global spatial distribution of various DMS oxidation products, including MSA and nss $SO_4^=$ [*Gondwe et al.*, 2003a, 2003b]. Model runs are made at a horizontal spatial resolution of $7.5^\circ \times 10^\circ$ for 19 vertically stacked layers extending up to the stratosphere. The model used is version 3 of the Tracer Model (TM3) [*Houweling et al.*, 1998; *Dentener et al.*, 1999, 2002; *Sciare et al.*, 2000b; *Jeuken et al.*, 2001; *Gondwe et al.*, 2003a, 2003b]. The model is state-of-the-art, contains comprehensive sulphur chemistry and can compute photochemical, heterogeneous, gas phase and aqueous phase transformation of chemical species. Dry and wet deposition is also considered.

[7] DMS chemistry as treated by TM3 has recently been extensively documented by *Gondwe et al.* [2003a, 2003b] and will not be repeated here. In short, however, DMS within the model is oxidized in the gas phase by photochemically produced hydroxyl radicals (OH) during daytime and photochemically destroyed gaseous nitrate radicals (NO_3) during nighttime or dark periods in polar regions. The products of the DMS-OH reaction within the model are MSA and SO_2 (sulphur dioxide), while only SO_2 is formed from NO_3 oxidation of DMS. MSA is removed from the atmosphere through wet and dry deposition [*Pszenny et al.*, 1990], while SO_2 undergoes oxidation by the OH radical, in the gas phase and during daytime, to form sulphuric acid (H_2SO_4) which in turn either condenses onto existing aerosols (heterogeneous nucleation), making them sulphate based, or nucleates with water vapour (binary homogeneous nucleation) to form new sulphate aerosols. Furthermore, SO_2 undergoes aqueous phase oxidation by H_2O_2 (hydrogen peroxide) and O_3 (ozone) within clouds also to form H_2SO_4, which further undergoes heterogeneous or homogeneous nucleation to form sulphate aerosols.

[8] MSA production in TM3 is temperature dependent (most effective under low ambient temperatures, with a maximum ambient temperature of 27°C [*Mauldin et al.*, 1999]) according to the kinetic information of *Hynes et al.* [1986]. The exact rate coefficient (cm^3 $molecules^{-1}$ s^{-1}) and its temperature dependence function used for MSA production by DMS + OH $\rightarrow$ 0.75 SO_2 + 0.25 MSA is $k_1M/(1. + k_2M)$, where $k_1 = 1.7 \times 10^{-42}\exp(7810./T)$, $k_2 = 5.5 \times 10^{-31}\exp(7460./T)$ and $M = O_2$ (molecules cm^{-3}) [*Hynes et al.*, 1986]. That used for DMS + OH $\rightarrow$ SO_2 + ... is $9.6 \times 10^{-12}\exp(-234/T)$ according to *Hynes et al.* [1986] and *Atkinson et al.* [1992] while that used for DMS + NO_3 $\rightarrow$ SO_2 + ... is $1.9 \times 10^{-13}\exp(520/T)$ according to *Atkinson*

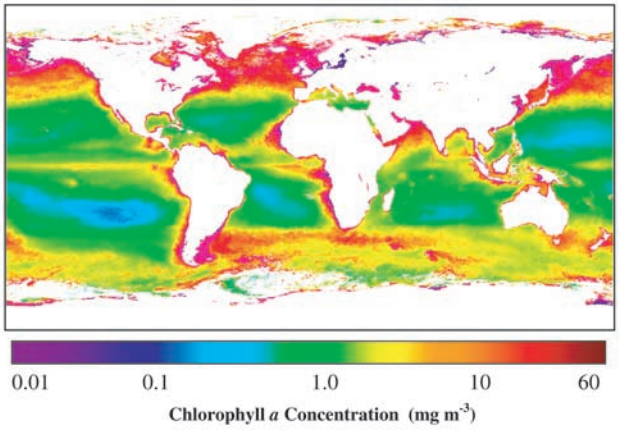

Figure 1. The 2002 mean annual geographical distribution and concentration of phytoplankton deduced from satellite-derived chlorophyll *a* at the ocean surface. The image is courtesy of NASA and is a product from the Moderate Resolution Imaging Spectroradiometer (MODIS) aboard the Terra and Aqua satellites.

et al. [1992]. Meteorological records from European Centre for Medium-Range Weather Forecasts (ECMWF) analyses for the year 1993 are used to determine the dynamics and chemical species transport within the model.

[9] In addition to its oceanic algal source, DMS also has terrestrial sources: wetlands, oxic fresh water lakes, alfalfa, ruminants [*Bates et al.*, 1992; *Spiro et al.*, 1992; *Hines et al.*, 1993; *Hobbs and Mottram*, 2000]. However, this source is small in comparison to its oceanic counterpart. The existence of the terrestrial source means that MSA measurements include both the oceanic and terrestrial signals. The same is true for nss $SO_4^=$, which also has both oceanic and terrestrial sources (anthropogenic and natural). As such, in this paper we show the ratio of MSA to nss $SO_4^=$ resulting from all their sources. In doing so, it is hoped that the model results will be as comparable as possible to observed MSA:nss $SO_4^=$ ratios, which also have a terrestrial, marine, anthropogenic, and natural signal. Published records of the ratio have been collated and compared to modeled ratios in Table 1. Ice core measurements of the ratio extracted from literature have also been included in Table 1. Since these are historical records and are measured within deposited snow and ice rather than in the atmosphere, they cannot directly be compared to modeled (atmospheric) results. However, we have chosen to show them anyway, since they add additional perspective on the spatial variation of the ratio (Arctic versus Antarctic regions) as well as the variation of the magnitude of the ratio over an historical time period.

[10] We also show the ratio of MSA to nss $SO_4^=$ resulting from only the oceanic DMS source. This is useful in determining the relative yields of MSA and nss $SO_4^=$ from the atmospheric oxidation of ocean-leaving DMS, at various locations during different periods. Comparisons to measurements are made (see Table 2) and allow evaluation of model performance in reproducing close-to-observed yields of MSA and nss $SO_4^=$. Differences between the results of the "oceanic source only" and "all sources" simulations inform on the impact of terrestrial sources on the observed MSA:nss $SO_4^=$ ratio.

[11] TM3 makes use of tagged tracers to identify or label the molecules of DMS originating from an oceanic source and subsequently the molecules of MSA and nss $SO_4^=$ produced from it. This allows the model to be run for all sources and emissions relevant to the chemistry of the sulphur cycle and at the same time allows the isolation of the MSA or nss $SO_4^=$ arising from any given source of interest. It is important to run the model for all sulphur sources, instead of considering DMS as the only sulphur source, since it allows a more realistic calculation of chemical species concentrations to take place. When all sulphur emissions are considered (instead of a single emission source) the oxidants calculated by the model are consumed by all possible chemical species that are oxidized by them. Such fair competition for oxidants is also the case in the real atmosphere.

[12] Additionally, all chemistry within TM3 is calculated online; hence the mean oxidant fields within the model depend on transport, the diurnal cycle, and their removal and formation sources. Changes in the removal mechanisms of oxidants (e.g., the omission of chemical species (other than DMS) consumed by OH) would feed back on the oxidant concentration simulated by the model. There is, therefore, a need to always simulate the total sulphur cycle and all chemical species relevant to it before isolating the final concentrations of selected chemical species within the cycle.

[13] Terrestrial and marine anthropogenic sources of sulphur used in TM3 include industrial, biomass burning, and transportation emissions from the EDGAR (Emission Database for Global Atmospheric Research) database [*Olivier and Berdowski*, 2001]. Terrestrial and marine natural sources include volcanic emissions [after *Andres and Kasgnoc*, 1998] and DMS emissions (after *Kettle et al.* [1999] for marine areas and *Spiro et al.* [1992] for terrestrial areas). TM3 uses the *Liss and Merlivat* [1986] model of air-sea exchange to transform the surface seawater DMS concentrations in the *Kettle et al.* [1999] database into emissions.

[14] Validation of TM3 output on MSA concentrations with published measurements has recently been made by *Gondwe et al.* [2003a, 2003b] and will not be repeated here. Similarly, *Jeuken et al.* [2001] have previously validated the capability of the TM3 model in simulating global 3-D nss $SO_4^=$ concentrations under a model setup similar to ours and for the same model year and will not be repeated here. Briefly, however, TM3 performed reasonably well in reproducing observed MSA measurements at most measurement stations globe-wide, with a general underestimation of 24% (degrees of freedom = 34). In terms of nss $SO_4^=$, the Intergovernmental Panel on Climate Change (IPCC) conducted a study [*IPCC*, 2001] intercomparing the performance of 11 global models in simulating close-to-observed sulphate concentrations. The TM3 is among the group of models which was evaluated. The model was found to overestimate sulphate concentrations by ~46%. In the current study we evaluate the performance of TM3 in simulating close-to-observed MSA:nss $SO_4^=$ ratios. Overall, model performance is fair (i.e., a general overestimation of 23%; degrees of freedom = 90) for MSA:nss $SO_4^=$ ratios resulting from all sources in areas where actual measure-

Table 1. Observed Versus Modeled MSA:nss $SO_4^=$ Ratios Resulting From all Modeled Sulphur Sources

Site	Period	MSA:nss $SO_4^=$ Ratio[a]		Reference[b]
		Observed Ratio	Modeled Ratio	
	Atmosphere			
Arctic	July–Aug 1986	0.017	0.290	LB, LI
	April 1986 to April 1987	0.007	0.108	LB, LI
	March–April 1988	0.003	0.060	LB, LI
Barrow, Alaska	March–April 1989	0.013	0.060	LI
Dye, Greenland	Aug. 1988 to July 1989	0.017	0.093	LI, DA
	April–May 1989	0.006	0.030	LI
	June–July 1989	0.063	0.180	LI
Summit, Greenland	June–July 1989	0.035	0.125	LI
	June–Aug. 1990	0.051	0.207	LI
	29 June to 9 July 1992	0.027	0.130	BG1
	25 May to 13 July 1993	0.014	0.072	BG2
Bering Sea	Aug. 1988	0.410	0.410	LI
Arctic Free Troposphere	July–Aug. 1988	0.011	0.065	LI
Above Arctic Pack Ice (73°N, 157°W)	July 1988	0.280	0.380	LI
North and South Atlantic				
North Atlantic (open ocean)	19 Aug. to 6 Sept. 1988	0.050	0.040	PZ2
Western North Atlantic	Sept. 1985 to Sept. 1986	0.033	0.038	BE3
Equatorial Atlantic	9 Oct. to 2 Nov. 1996	0.028	0.120	SR
Miami	July 1991 to March 1993	0.020	0.038	PR2
South Florida	Aug. 1978, May–July 1979, Aug. 1981	0.013	0.038	SZ1
Barbados	July 1989 to March 1993	0.030	0.110	GA, PR2, SV5
Bermuda	July 1989 to March 1993	0.020	0.056	GA, PR2, SV5
Heimaey, Iceland	July 1991 to March 1993	0.060	0.085	PR2
Mace Head, Ireland	July 1989 to March 1993	0.040	0.052	GA, PR2
	Aug. 1989 to Aug. 1990	0.054	0.052	SV5
	June–July 1994	0.170	0.125	MC
United Kingdom	1988–1990	0.012	0.048	DH
Tenerife	July 1991 to March 1993	0.010	0.043	PR2
	April 1989 to April 1993	0.005	0.043	SV5
Eastern Mediterranean (Greece)	Oct. 1996 to Sept. 1999	0.010–0.170	0.038	KM
Temperate South Atlantic	9 Oct. to 2 Nov. 1996	0.100	0.120	SR
Tropical South Atlantic	Feb.–March 1991	0.066	0.093	AN
North Pacific				
Northeast Pacific	May 1987	0.050	0.030	BA
Midway Island	1981–1987	0.050	0.071	SV1, SZ1, SZ3
Equatorial Pacific				
	Feb.–March 1991	0.070	0.140	HU
Fanning Island	1981–1987	0.065	0.178	SP, SV1, SZ1, SZ2, SZ3
South Pacific				
American Samoa	1981–1987	0.065	0.205	PR2, SP, SV1, SV4, SV5, SZ2, SZ3
Norfolk Island	1983–1987	0.100	0.162	SV1, SZ3
New Caledonia	1983–1987	0.050	0.093	SV1, SZ3
Leigh, New Zealand	1991, 1992	0.010–0.210	0.165	WM
Indian Ocean				
Somalia Coast	Feb. –May 1979	0.036	0.053	SZ1
Southern Ocean plus Antarctic				
Drake Passage	22–27 March 1986	1.010	0.580	BE1
	21 March to 27 April 1986	0.650	0.480	PZ1
Gerlache Strait	April 1986	0.600	0.530	BE1
Antarctic coastal shelf (Gerlache Strait)	17–21 April 1986	1.860	0.530	BE1
Palmer	Jan.–Feb. 1994	0.610	0.850	BE4, JF
	April 1990 to June 1991	0.500	0.452	SV3
Mawson	Feb. 1987 to Jan. 1992	0.220	0.651	PR1, PR2, SV2, SV3
	1987–1991	0.214	0.651	MI, LP
	Jan. 1987–1991	0.230	0.710	LP
	Feb. 1987–1991	0.241	0.800	LP
	March 1987–1991	0.310	1.010	LP
	April 1987–1991	0.320	1.060	LP
	May 1987–1991	0.160	0.270	LP
	June 1987–1991	0.100	0.130	LP
	July 1987–1991	0.060	0.090	LP
	Aug. 1987–1991	0.060	0.370	LP

Table 1. (continued)

Site	Period	MSA:nss $SO_4^=$ Ratio[a]		Reference[b]
		Observed Ratio	Modeled Ratio	
	Sept. 1987–1991	0.120	1.040	LP
	Oct. 1987–1991	0.160	1.120	LP
	Nov. 1987–1991	1.180	1.010	LP
	Dec. 1987–1991	0.240	0.870	LP
Ross Island	Jan. 1992	0.197–0.298	0.640	WY
Cape Grim	Aug. 1976 to June 1984	0.064	0.103	AY1
	Nov. 1988 to Feb. 1992 mid-winter	0.060	0.090	AY2, GI
	Nov. 1988 to Feb. 1992 mid-summer	0.180	0.160	AY2, GI
Southern Ocean, off Cape Grim	Dec. 1986	0.080–0.530	0.260	BE2
Dumont D'Urville	1991–1996	0.136 (0.015–0.323)	0.870	MI, LP
	Jan. 1994	0.040–0.300	0.850	LP
	Jan. (1991–1996)	0.184	0.850	MI, LP
	Feb. (1991–1996)	0.238	0.960	MI, LP
	March (1991–1996)	0.225	1.300	MI, LP
	April (1991–1996)	0.164	0.850	MI, LP
	May (1991–1996)	0.100	0.330	MI, LP
	June (1991–1996)	0.033	0.130	MI, LP
	July (1991–1996)	0.028	0.120	MI, LP
	Aug. (1991–1996)	0.031	0.290	MI, LP
	Sept. (1991–1996)	0.058	0.690	MI, LP
	Oct. (1991–1996)	0.070	1.370	MI, LP
	Nov. (1991–1996)	0.096	1.200	MI, LP
	Dec. (1991–1996)	0.123	1.220	MI, LP
Neumayer	1983–1995	0.252, (0.039–0.448)	0.790	MI, LP
	Jan. (1983–1994)	0.407	0.780	MI, LP
	Feb. (1983–1994)	0.308	0.880	MI, LP
	March (1983–1994)	0.400	1.010	MI, LP
	April (1983–1994)	0.229	0.850	MI, LP
	May (1983–1994)	0.111	0.190	MI, LP
	June (1983–1994)	0.075	0.110	MI, LP
	July (1983–1994)	0.062	0.150	MI, LP
	Aug. (1983–1994)	0.065	0.370	MI, LP
	Sept. (1983–1994)	0.111	0.870	MI, LP
	Oct. (1983–1994)	0.122	1.490	MI, LP
	Nov. (1983–1994)	0.129	0.830	MI, LP
	Dec. (1983–1994)	0.295	0.960	MI, LP
Halley	1991–1993	0.300 (0.045–0.535)	0.720	MI, LP
	Jan. (1991, 1993)	0.374	0.920	MI, LP
	Feb. 1991	0.329	0.800	MI, LP
	March 1991	0.433	0.720	MI, LP
	April 1991	0.291	0.850	MI, LP
	May 1991	0.118	0.190	MI
	June 1991	ND	0.110	MI, LP
	July 1991	ND	0.150	MI, LP
	Aug. 1991	ND	0.370	MI, LP
	Sept. 1991	0.100	0.870	MI
	Oct. 1991	0.104	1.370	MI, LP
	Nov. 1992	0.078	0.740	MI, LP
	Dec. 1992	0.280	1.040	MI, LP
	Ice Cores (Most Recent Period) and Surface Snow			
Arctic				
Renland, Greenland	historical record	0.060	-	HS
South Central Greenland	historical record	<0.050	-	WH
Summit, Greenland	historical record	~0.060	-	LE3
Central Greenland	historical record	~0.080	-	SZ4
Dye	Aug. 1988 to July 1989	0.010	-	DA
Antarctic				
Dolleman Island	historical record	0.460	-	MV, PR1
	historical record	0.382	-	MI2
	historical record	0.220	-	PA
Dominion Range	historical record	~0.050	-	PR1
Gomez	historical record	0.370	-	MV, MI2
Dyer	historical record	0.320	-	MV
Law Dome	historical record	0.390	-	IV
	historical record	0.177	-	MI2
Vostok	historical record	~0.050	-	LE1, MI2
South Pole	historical record (fall-winter)	~0.180	-	LE2
	historical record (spring-summer)	~0.125	-	LE2
	historical record	0.130	-	DE, MI2

Table 1. (continued)

Site	Period	MSA:nss $SO_4^=$ Ratio[a]		Reference[b]
		Observed Ratio	Modeled Ratio	
D10 (Terre Adélie)	historical record	0.030–1	-	SL
Filchner-Ronne Ice Shelf (Site 5)	1939–1989	0.059	-	MI1, MI2
Filchner-Ronne Ice Shelf (Site 6)	1936–1989	0.080	-	MI1, MI2
Filchner-Ronne Ice Shelf (Site D131)	1966–1989	0.192	-	MI1, MI2
Filchner-Ronne Ice Shelf (Site D136)	1962–1989	0.166	-	MI1, MI2
Filchner-Ronne Ice Shelf (Site D230)	1967–1989	0.189	-	MI1, MI2
Filchner-Ronne Ice Shelf (Site D231)	1965–1987	0.244	-	MI1, MI2
Filchner-Ronne Ice Shelf (Site D235)	1968–1987	0.181	-	MI1, MI2
Filchner-Ronne Ice Shelf (Site D236)	1965–1989	0.189	-	MI1, MI2
Filchner-Ronne Ice Shelf (Site D240)	1975–1982	0.222	-	MI1, MI2
Filchner-Ronne Ice Shelf (Site D330)	1966–1987	0.134	-	MI1, MI2
Filchner-Ronne Ice Shelf (Site D335)	1966–1987	0.193	-	MI1, MI2
Filchner-Ronne Ice Shelf (Site D336)	1964–1981	0.147	-	MI1, MI2
Filchner-Ronne Ice Shelf (Site D340)	1968–1982	0.162	-	MI1, MI2
Filchner-Ronne Ice Shelf (Site D341)	1956–1982	0.138	-	MI1, MI2
Dome C	historical record	0.031	-	MI2
Byrd	historical record	0.183	-	MI2
Berkner N	historical record	0.170	-	MI2
Berkner S	historical record	0.193	-	MI2
Ekstrøm 040	historical record	0.110	-	MI2
Ekstrøm 070W	historical record	0.097	-	MI2
Ekstrøm 090	historical record	0.098	-	MI2

[a]Where a range is given, the values correspond to a minimum and maximum. A single value represents a mean. ND = undetermined values due to MSA concentrations being below detection limit. The predicted ratios in the surface model layer are >1 in some areas due to the additional input of MSA from overlying and neighboring model layers. Runs were conducted for a total of 19 vertically stacked layers extending up to the stratosphere. The data used are only those measurements of total (i.e., no size cut) aerosol.

[b]AY1 = *Ayers et al.* [1986]; AY2 = *Ayers et al.* [1991]; AN = *Andreae et al.* [1995]; BA = *Bates et al.* [1990]; BE1 = *Berresheim* [1987]; BE2 = *Berresheim et al.* [1990]; BE3 = *Berresheim et al.* [1991]; BE4 = *Berresheim et al.* [1998]; BG1 = *Bergin et al.* [1994]; BG2 = *Bergin et al.* [1995]; DA = *Davidson et al.* [1993a]; DE = *Delmas et al.* [2003]; DH = *Davison and Hewitt* [1992]; GA = *Galloway et al.* [1993]; GI = *Gillett et al.* [1993]; HS = *Hansson and Saltzman* [1993]; HU = *Huebert et al.* [1993]; IV = *Ivey et al.* [1986]; JF = *Jefferson et al.* [1998]; KM = *Kouvarakis and Mihalopoulos* [2002]; LB = *Li and Barrie* [1993]; LE1 = *Legrand et al.* [1991]; LE2 = *Legrand et al.* [1992]; LE3 = *Legrand et al.* [1997]; LP = *Legrand and Pasteur* [1998]; LI = *Li et al.* [1993]; MI1 = *Minikin et al.* [1994]; MI2 = *Minikin et al.* [1998]; MC = *McArdle et al.* [1998]; MV = *Mulvaney et al.* [1992]; PA = *Pasteur et al.* [1995]; PR1 = *Prospero et al.* [1991]; PR2 = *Prospero et al.* [1995]; PZ1 = *Pszenny et al.* [1989]; PZ2 = *Pszenny et al.* [1990]; SL = *Saigne and Legrand* [1987]; SP = *Savoie and Prospero* [1989]; SR = *Sciare et al.* [2000a]; SV1 = *Savoie et al.* [1989]; SV2 = *Savoie et al.* [1992]; SV3 = *Savoie et al.* [1993]; SV4 = *Savoie et al.* [1994]; SV5 = *Savoie et al.* [2002]; SZ1 = *Saltzman et al.* [1983]; SZ2 = *Saltzman et al.* [1985]; SZ3 = *Saltzman et al.* [1986]; SZ4 = *Saltzman et al.* [1997]; WH = *Whung et al.* [1994]; WM = *Wylie and de Mora* [1996]; WY = *Wylie et al.* [1993].

ments of the ratio have been made (i.e., the Atlantic Ocean, Pacific Ocean, Indian Ocean, Southern Ocean, Antarctica, and the Arctic). However, the model-observation comparisons for the MSA:nss $SO_4^=$ ratio derived solely from the oceanic DMS source are not as satisfactory (an overall overestimation of a factor of 3; degrees of freedom = 50). Model performance for individual regions is given and discussed in appropriate sections of section 3 below.

3. Results and Discussion

3.1. Ratios Considering All Sulphur Sources

[15] Here we report results on MSA:nss $SO_4^=$ ratios which were calculated considering the contribution from all sulphur sources in the TM3 model (i.e., anthropogenic (industrial, transportation, and other), volcanic, DMS (oceanic and terrestrial), and other natural and biogenic sources).

[16] Measured data in Table 1 have been obtained from literature focusing on the MSA:nss $SO_4^=$ ratio and those which did not focus on the ratio but reported concurrent measurements of MSA and nss $SO_4^=$. Only those measurements which have been corrected for excess sulphate have been included in this study. Furthermore, only those measurements that include the total (sub- and super-micron) aerosol have been considered (i.e., those that considered them individually [e.g., *Turekian et al.*, 2001] have been excluded). Studies which distinguished their measurements on the basis of air mass origin [e.g., *Galloway et al.*, 1990]

Table 2. Observed Versus Modeled Atmospheric MSA:nss $SO_4^=$ Ratios Resulting Solely From the Oceanic DMS Source of the Two Compounds

Site	Period	MSA:nss $SO_4^=$ Ratio[a]		Reference[b]
		Observed Ratio	Modeled Ratio	
North Atlantic				
Barbados	19 Aug. to 6 Sep 1988	0.054	0.240	SA
Bermuda	Sept. 1985 to Sept. 1986	0.057	0.240	SA
Tenerife	9 Oct. to 2 Nov. 1996	0.050	0.240	SA
Mace Head, Ireland	May–Aug. 1989–1990	0.227[c]	0.330	SA
	Oct.–March 1989–1990	0.015[c]	0.210	SA
	Aug. 1988 to July 1991	0.049[d]	0.320	SA
	June–July 1994	0.670[d]	0.360	MA
Antarctic				
Dumont D'Urville	1991–1996	0.162 (0.014–0.412)	0.790	LP[e]
	Jan. (1991–1996)	0.174	0.680	LP[e]
	Feb. (1991–1996)	0.248	0.950	LP[e]
	March (1991–1996)	0.276	1.300	LP[e]
	April (1991–1996)	0.234	0.960	LP[e]
	May (1991–1996)	0.266	0.370	LP[e]
	June (1991–1996)	0.120	0.280	LP[e]
	July (1991–1996)	0.110	0.230	LP[e]
	Aug. (1991–1996)	0.065	0.400	LP[e]
	Sept. (1991–1996)	0.075	0.890	LP[e]
	Oct. (1991–1996)	0.140	1.370	LP[e]
	Nov. (1991–1996)	0.100	1.160	LP[e]
	Dec. (1991–1996)	0.138	0.920	LP[e]
Neumayer	1983–1994	0.227 (−0.062–0.547)	0.790	LP[e]
	Jan. (1983–1994)	0.460	0.750	LP[e]
	Feb. (1983–1994)	0.325	0.950	LP[e]
	March (1983–1994)	0.286	1.300	LP[e]
	April (1983–1994)	0.267	1.070	LP[e]
	May (1983–1994)	0.190	0.310	LP[e]
	June (1983–1994)	0.140	0.280	LP[e]
	July (1983–1994)	0.117	0.230	LP[e]
	Aug. (1983–1994)	0.104	0.500	LP[e]
	Sept. (1983–1994)	0.170	1.100	LP[e]
	Oct. (1983–1994)	0.190	1.500	LP[e]
	Nov. (1983–1994)	0.160	0.700	LP[e]
	Dec. (1983–1994)	0.320	0.920	LP[e]
Halley	Feb. 1991 to Jan. 1993	−0.070–0.770	0.790	LP[e]
	Jan. (1991, 1993)	0.490	0.890	LP[e]
	Feb. 1991	0.240	0.950	LP[e]
	March 1991	0.380	0.990	LP[e]
	April 1991	0.400	0.960	LP[e]
	May 1991	ND[f]	0.280	LP[e]
	June 1991	ND[f]	0.220	LP[e]
	July 1991	ND[f]	0.230	LP[e]
	Aug. 1991	ND[f]	0.400	LP[e]
	Sept. 1991	ND[f]	1.930	LP[e]
	Oct. 1991	0.220	1.500	LP[e]
	Nov. 1992	0.160	0.700	LP[e]
	Dec. 1992	0.390	0.920	LP[e]
Mawson	1987–1991	0.250	1.020	LP[e]
	Jan. 1987–1991	0.250	0.750	LP[e]
	Feb. 1987–1991	0.280	0.870	LP[e]
	March 1987–1991	0.360	1.140	LP[e]
	April 1987–1991	0.435	1.180	LP[e]
	May 1987–1991	0.270	0.430	LP[e]
	June 1987–1991	0.210	0.280	LP[e]
	July 1987–1991	0.170	0.230	LP[e]
	Aug. 1987–1991	0.110	0.550	LP[e]
	Sept. 1987–1991	0.170	1.100	LP[e]
	Oct. 1987–1991	0.230	1.240	LP[e]
	Nov. 1987–1991	0.230	1.070	LP[e]
	Dec. 1987–1991	0.260	0.920	LP[e]

[a]Data used are only those measurements of total (i.e., no size cut) aerosol.
[b]LP = *Legrand and Pasteur* [1998]; MA = *McArdle et al.* [1998]; SA = *Savoie et al.* [2002].
[c]When antimony is the anthropogenic tracer.
[d]When aerosol nitrate is the anthropogenic tracer.
[e]Before calculation of ratios, nss $SO_4^=$ was corrected for a non-DMS contribution of 15 ± 5 ng m^{-3} in winter and 27 ± 13 ng m^{-3} in summer. Samples from periods soon after major volcanic eruptions (Nov. 1991 to Oct. 1992) were not included in the analysis.
[f]ND = undetermined values due to MSA concentrations being below detection limit.

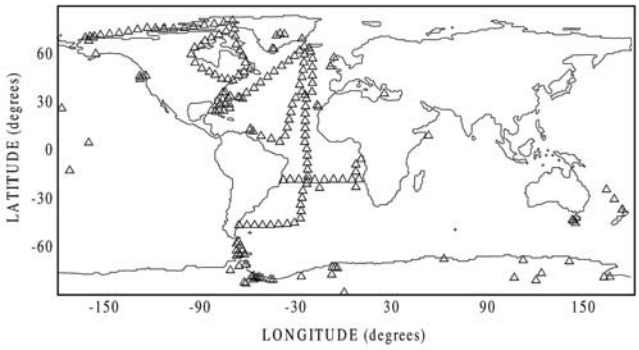

Figure 2. Location of sites where MSA:nss $SO_4^=$ ratio measurements are available. Ship transects are also shown. Data from these sites are compared to modeled values in Tables 1 and 2. The data used from these sites are only those measurements of total (i.e., no size cut) aerosol.

are not included in model-observation comparisons either. Ice core records of the ratio have also been included at the end of Table 1. While we cannot present similar modeled data for comparison, the inclusion of these ice core data is useful in comparing the magnitude and consistency of ice core data on the MSA:nss $SO_4^=$ ratio with atmospheric measurements. Since large-scale atmospheric circulation and processes supply geochemical tracers to an ice sheet over time, ice cores contain historical records which may provide information and insight on past and present atmospheric composition, chemistry, and dynamics.

[17] Comparison of measured versus modeled ratios in Table 1 shows fair model performance (mainly within a factor of 2) over the Indian Ocean, North and South Pacific, Southern Ocean and Antarctica, North and South Atlantic Ocean, Gerlache Strait, Drake Passage, Palmer, and Cape Grim. Comparison of observed and modeled ratios at Halley, Neumayer, and Dumont D'Urville stations on Antarctica at monthly scales shows excessive overprediction. However, at the annual scale this is less dramatic, certainly for Halley and Neumayer (overprediction by factors of 2 and 3, respectively). The Antarctic coastline is characterized by extremely sharp meridional gradients of the MSA:nss $SO_4^=$ ratio, with the position of specific isolines changing dramatically from month to month. This is probably driven by similarly sharp tropospheric temperature gradients along the coastline, which are in turn initiated by contrasts in temperatures between the relatively warmer ocean to the north and cold ice shelves to the south [*Parish and Bromwich*, 1991; *König-Langlo et al.*, 1998]. Even a slight displacement of specific isolines in the model year versus the measurement years can lead to discrepancies between the ratios simulated for a given coastal Antarctic location.

[18] In the Northern Hemisphere, MSA production is generally overpredicted above the Arctic region. Both long- and short-term observations of the ratio at Dye in Greenland are overpredicted by approximately a factor of 5, while those at Alert in Canada are overpredicted by approximately a factor of 15. Model performance above the Bering Sea is good but could be coincidental as the measurement record is too short to confirm this (only 1 month long). Despite such overprediction at some locations, seasonal variability in the MSA:nss $SO_4^=$ ratio is nicely captured by the model at most stations (see Figure 3).

[19] Differences between the simulated and measured MSA:nss $SO_4^=$ ratio over Greenland may arise for various reasons. *Bergin et al.* [1994] report that fog occurs throughout the year, with the highest frequencies occurring typically during winter at Dye, and during spring and summer at Summit in central Greenland. Fog may facilitate aqueous phase formation of nss $SO_4^=$. The model resolution selected for this study may have been too coarse to resolve most local fog events at these sites, and this might have resulted in the underestimation of nss $SO_4^=$ production over Greenland. Comparatively, MSA formation occurs in the gas phase and is not affected by this. The overall result is an increase in the modeled MSA:nss $SO_4^=$ ratio in contrast to a low observed ratio.

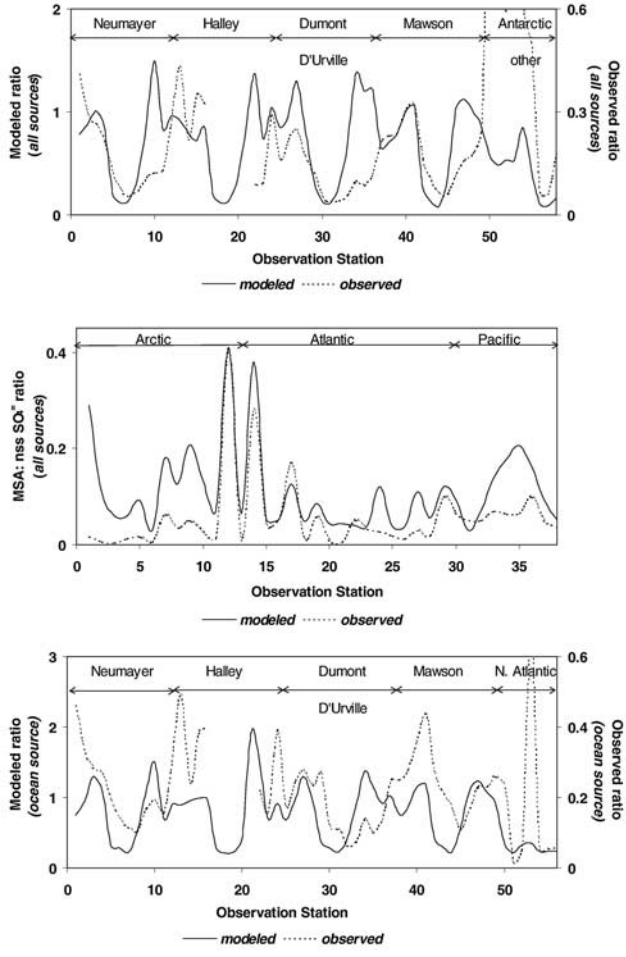

Figure 3. Observed versus modeled MSA:nss $SO_4^=$ ratio. This is a graphed version of Tables 1 and 2. Note the different scales for the modeled and observed data due to an overall model overestimation of ~23% (degrees of freedom = 90) for ratios resulting from all sources and a factor of 3 (degrees of freedom = 50) for ratios resulting from the oceanic DMS source alone.

[20] Not only does fog facilitate nss $SO_4^=$ formation, but it also facilitates the scavenging of hygroscopic atmospheric aerosols and their subsequent wet deposition [*Bergin et al.*, 1994]. On the basis of both long- and short-term measurements, *Li et al.* [1993] and *Davidson et al.* [1993a, 1993b] have suggested the removal of MSA by precipitation as one of the major factors controlling the seasonal distribution of MSA in the Arctic atmosphere. Again the coarse model resolution and the consequent inadequate determination of local fog events might have reduced the removal of MSA, relative to nss $SO_4^=$, in the model, resulting in a high modeled MSA:nss $SO_4^=$ ratio. While nss $SO_4^=$ is also removed by wet deposition, precipitation scavenging of MSA is somewhat greater due to its typically larger size [*Wylie and De Mora*, 1996; *O'Dowd et al.*, 1997; *Berresheim et al.*, 1998]. Increased dry deposition (gravitational settling) further results in a shorter lifetime for the heavier MSA [*Bergin et al.*, 1995]. This can affect the magnitude of the MSA:nss $SO_4^=$ ratio in areas of enhanced atmospheric subsidence and precipitation [*Li et al.*, 1993; *Huebert et al.*, 1993; *Turekian et al.*, 2001].

[21] The fact that the MSA:nss $SO_4^=$ ratios [*Li et al.*, 1993] were measured in a different year to the model year may also have resulted in discrepancies in the spatial variation of precipitation events which in turn have possibly led to reduced MSA removal in the vicinity of some sampling stations in the Arctic within the model. Furthermore, a possibility exists that, for the model year of 1993, MSA was advected from sources above the Northern Hemispheric oceans into the Arctic region which raised the predicted MSA concentrations in this area. Back trajectories calculated for Dye in Greenland have previously revealed strong influences of surrounding areas on the total aerosol mass in this region [*Davidson et al.*, 1985, 1993a, 1993b; *Bergin et al.*, 1994]. Also, the selection of a different MSA versus SO_2 yield function, for the MSA production reaction in the model Arctic atmosphere, might have led to better agreement between simulated and observed MSA.

[22] In general, a review of the spatial distribution of the measured MSA:nss $SO_4^=$ ratio presented in Table 1 confirms that the ratio is highest around the polar regions and lowest within the tropics. However, while such comparisons of the ratio between the hot low latitudes, temperate midlatitudes, and cold high latitude regions support the temperature-dependence theory of the MSA production mechanism [also *Ayers et al.*, 1996; *Campolongo et al.*, 1999; *Mauldin et al.*, 1999], this theory has been observed to be less effective on a seasonal scale at high latitudes, when the MSA:nss $SO_4^=$ ratio was highest in summer and lowest in winter (e.g., *Ayers et al.* [1986, 1991, 1996]; *Gillett et al.* [1993] at Cape Grim in Australia; *Savoie and Prospero* [1989] at North Pacific measurement stations; *Savoie et al.* [2002] at Mace Head in Ireland; *Prospero et al.* [1991] at Mawson on Antarctica; *Savoie et al.* [1993] at Palmer, Mawson, and Marsh on Antarctica; *Legrand and Pasteur* [1998] and *Minikin et al.* [1998] at Neumayer, Dumont d'Urville, and Mawson in Antarctica; *Wylie and De Mora* [1996] at Leigh in New Zealand; *McArdle and Liss* [1995] at Mace Head in Ireland and Ny Ålesund in Spitsbergen; *McArdle et al.* [1998] at Plynlimon in Wales and Mace Head in Ireland; *Li and Barrie* [1993] and *Li et al.* [1993] at Alert in Canada and Barrow in Alaska; *Davidson et al.* [1993a] and *Jaffrezo et al.* [1994] at Dye in Greenland). A similar seasonality is reported for the ratio measured in near-surface firn and ice core layers [*Mulvaney et al.*, 1992; *Mulvaney and Wolff*, 1994] and surface snow [*Davidson et al.*, 1993a; *Legrand and Pasteur*, 1998] in Antarctica. The reduced marine biological activity and low seawater DMS conditions in winter at high latitudes have been cited as the probable cause of the reduced effectiveness of the temperature dependence of the MSA production mechanism [*Minikin et al.*, 1998; *Legrand and Pasteur*, 1998]. We further propose that due to the longer day length in summer, DMS oxidation by the photochemically produced OH (to form MSA) is enhanced. Comparatively, despite temperatures being low (and, therefore, favorable for MSA production), less OH availability in the dark winter months at high latitudes results in suppressed DMS oxidation (MSA formation). Temperature alone is, therefore, not the only important factor in MSA formation at high latitudes. Light conditions also are important. Lower season-induced temperature amplitudes in the tropical and subtropical atmosphere and continued marine biogeochemical activity comparatively result in a negligible seasonal variation in the MSA:nss $SO_4^=$ ratio in this region [*Saltzman et al.*, 1986; *Savoie and Prospero*, 1989; *Berresheim et al.*, 1991; *Huebert et al.*, 1993; *Savoie et al.*, 1994, 2002].

[23] Our model results show trends similar to those measured, with the highest MSA:nss $SO_4^=$ ratios occurring with increasing latitude (Table 1). Furthermore, the governance of light conditions rather than temperature, above seasonal trends at high latitudes, are also well reproduced by the TM3 model, with the highest MSA:nss $SO_4^=$ occurring in summer rather than in winter (Figures 4, 5a, and 5b). *Li et al.* [1993] found that the MSA:nss $SO_4^=$ ratios in the Arctic atmosphere are highly variable seasonally (with minima in winter and maxima in summer). TM3 model results are in agreement with this observation (Figures 5a and 5b).

[24] Measurements of the MSA:nss $SO_4^=$ ratio in the North and equatorial Pacific are coherent with one another (Table 1). Measurements in the Caribbean and the United States east coast also agree in magnitude (Table 1). Long-term observations of the ratio in the South Pacific are similarly consistent in magnitude with one another (Table 1). TM3 model reproduction of measured ratios in these regions is fair (around a factor of 2).

[25] Generally, comparison of the measured ice core versus atmospheric MSA:nss $SO_4^=$ ratios over the Arctic shows similarities in magnitude of the ratio over different sampling stations (Table 1). In contrast, the ice core record-derived ratios for Antarctica are slightly lower than those derived from atmospheric measurements over the same area (Table 1). Shortcomings in the analytical determination of MSA in polar ice may lead to this discrepancy. In addition, studies by *Wagnon et al.* [1999] and *Delmas et al.* [2003] could offer further explanation. Measurements carried out in firn layers over various locations on Antarctica by these authors suggest that the deposition of MSA is reversible. Their results suggest a considerable release of deposited MSA to the interstitial firn air, which is then lost to the atmosphere (if in upper firn layers) or is entrapped in air bubbles when the firn is transformed into ice in deeper layers. The fact that MSA released

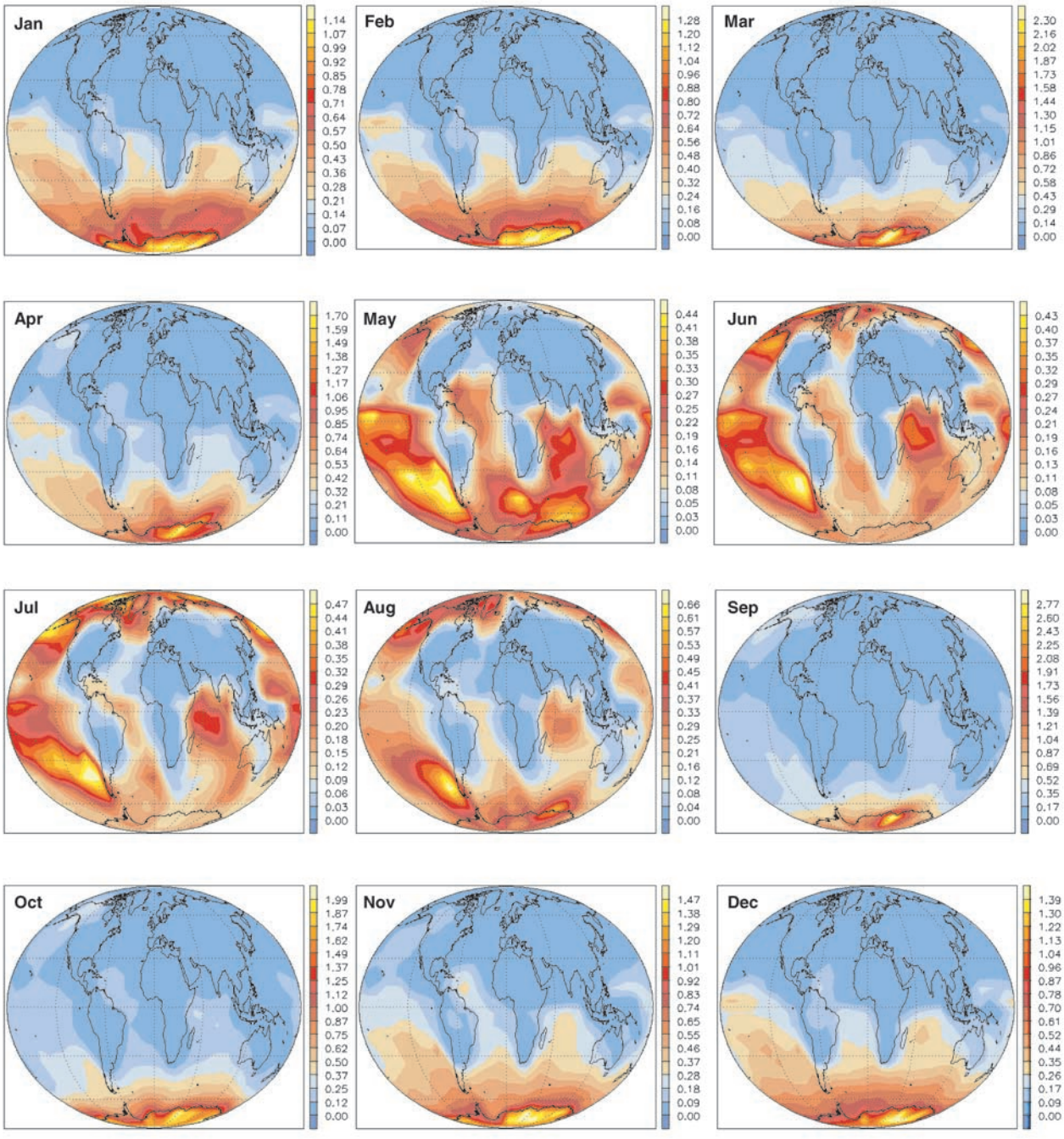

Figure 4. Global monthly mean surface (~1009 hPa) distribution of TM3-modeled MSA:nss $SO_4^=$ ratio as derived from all sulphur sources input into the model. The predicted ratios in the surface model layer are >1 in some areas due to the additional input of MSA from overlying and neighboring model layers. Runs were conducted for a total of 19 vertically stacked layers extending up to the stratosphere.

to the gaseous phase is not taken into account in chemical analysis of firn cores, as well as that it may be lost from firn samples during storage, may lead to the lower MSA values observed in upper level core samples versus the atmosphere above it. It is peculiar, however, that the loss of MSA to the interstitial firn air is not equally evident in comparisons between Arctic air versus ice core derived ratios in Table 1.

[26] The results of ice core analyses by *Mulvaney et al.* [1992], *Kreutz et al.* [1998], and *Pasteur and Mulvaney* [1999, 2000] could also explain the rather low correspondence between ice core-derived ratios and atmospheric-derived ratios in Antarctica. These authors have observed the migration of MSA from summer ice core layers, where it is initially deposited, to winter layers at various Antarctic

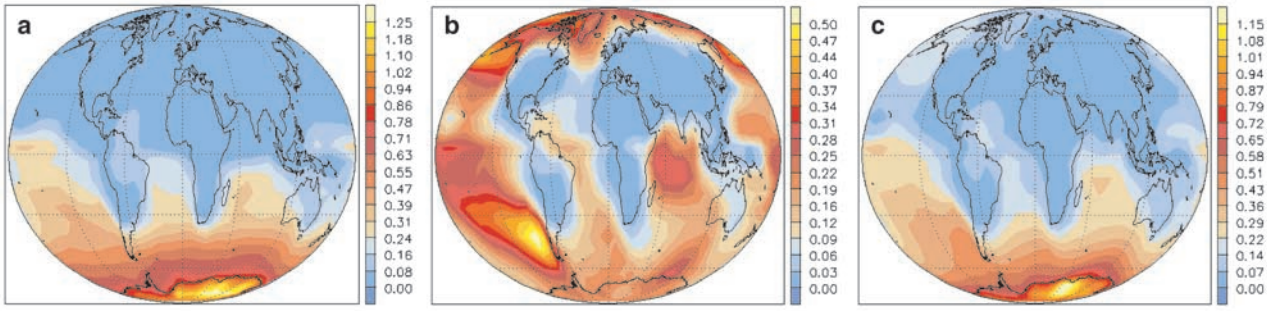

Figure 5. (a) December–January–February mean surface (~1009 hPa) distribution of TM3-modeled MSA:nss $SO_4^=$ ratio; (b) as in Figure 5a but for June–July–August; (c) as in Figure 5a but for an annually averaged period.

measurement stations. In contrast, no migration of nss $SO_4^=$ was observed. Such relocation of MSA relative to nss $SO_4^=$ can affect the MSA:nss $SO_4^=$ ratio deduced from different sections of an ice core and make the ratio obtained in deep ice different from its initial value at deposition. The ratio derived from an ice core at a particular location may also, therefore, become inconsistent with that observed in the atmosphere above it.

[27] In addition, *Wolff et al.* [1998] have pointed out that blowing snow and the redistribution of surface snow by drifting can also affect the MSA:nss $SO_4^=$ ratio in several ways. First, blowing snow (which was observed to occur at least 33% of the time during winter at station South Pole [*Harder et al.*, 1996]) can scavenge particles from the lower atmosphere and correspondingly increase their concentration in deposited ice, with the scavenging ratio for nss $SO_4^=$ being slightly higher than that for MSA [*Wolff et al.*, 1998]. Second, drifting of deposited snow can lead to redistribution of snow upwind to a new location, thus increasing concentrations in the new location and removing a snowfall record in the location of original deposition. Drifting snow was reported in >40% of all meteorological observations at Neumayer; 13% at Dumont D'Urville; and 18% at Halley in Antarctica [*Wolff et al.*, 1998], and so its modulating effect on MSA:nss $SO_4^=$ ratios in the Antarctic region can be quite significant. Both these reasons can lead to a distorted spatial distribution record of the MSA:nss $SO_4^=$ in ice as well as cause a mismatch between atmospheric-observed ratios and those observed in ice cores below a given location.

[28] Overall however, in terms of magnitude, the ice core derived ratio exhibits more consistency while the atmospheric record shows more variability. Simultaneous measurements of MSA and nss $SO_4^=$ air and fresh snow by *Davidson et al.* [1993a] led to the same conclusion. Differences in the length of sampling time may be a cause of this effect, with ice core records representing longer sampling times, and, therefore, data smoothing, than their atmospheric counterparts. In addition, MSA may condense on small or large particles, depending on the cleanness of an air mass. If it condenses on large particles, MSA may have a shorter atmospheric lifetime due to increased deposition potential. The passage of air masses of different air quality from time to time may, therefore, cause variability in the magnitude of the MSA:nss $SO_4^=$ ratio observed in the atmosphere of a given location over time.

[29] Comparison of ice core MSA:nss $SO_4^=$ ratios shows that the ratios in the Greenland area are in good agreement with one another, as are those over Antarctica, and that in general, ice core records of the ratio over the Arctic are lower than those over Antarctica (Table 1). This is in agreement with the TM3 model findings of lower atmospheric MSA:nss $SO_4^=$ ratios in the Northern Hemisphere than in the Southern Hemisphere (Figure 5c).

[30] Overall, measured and modeled MSA:nss $SO_4^=$ ratios show higher values at southern middle and high latitudes than at northern ones (Table 1, Figures 4 and 5c). Seawater DMS concentrations measured by *Huebert et al.* [1993] along a transect during a research ship cruise in the equatorial Pacific, during February and March, maximized toward the south rather than the north. Accordingly, these authors observed slightly higher MSA:nss $SO_4^=$ ratios to the south of the transects than to the north, in agreement with the model calculations of *Kreidenweis et al.* [1991], who found the ratio to be higher at southern latitudes than at northern ones during January. Our model results similarly show that the ratio during these months is highest in the Southern Hemisphere, where it is summer (Figures 4 and 5a).

[31] Analysis of the horizontal spatial distribution of the modeled MSA:nss $SO_4^=$ ratios (Figures 4 and 5a) shows that the highest ratios occur in the Southern Hemisphere throughout the year and that even in the austral winter, the Southern Hemisphere does not relinquish its monopoly of high MSA:nss $SO_4^=$ ratios. This is in agreement with *Gondwe et al.* [2003a, 2003b], who found that the contribution of ocean-leaving DMS to the annually averaged atmospheric burdens of DMS oxidation products is greatest in the Southern Hemisphere. Unlike the Southern Hemisphere, the Northern Hemisphere is a region in which the atmospheric sulphur cycle is dominated by anthropogenic inputs throughout the whole year. This results in a reduced MSA:nss $SO_4^=$ ratio in the Northern Hemisphere. Only during summer do marine biogenic sources in the Northern Hemisphere contribute a noteworthy yet minor fraction of the atmospheric sulphate (see Figures 4 and 5). This finding is in agreement with short- and long-term measurements in the Arctic atmosphere by *Li et al.* [1993].

[32] Model calculations show a maximum in the MSA:nss $SO_4^=$ ratio at atmospheric layers above the boundary layer around Antarctica during most of the year (not shown, but

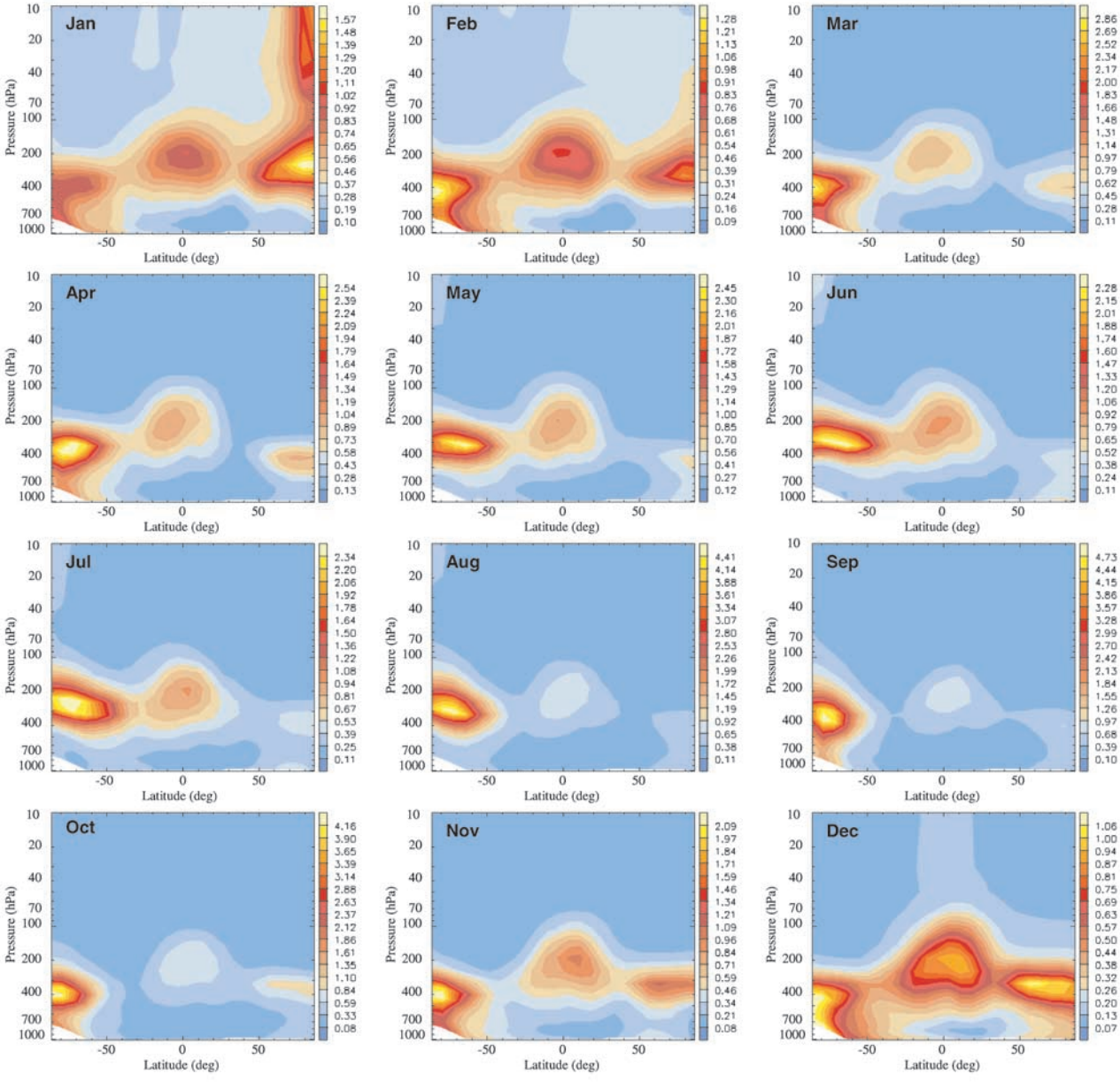

Figure 6. Modeled zonal monthly mean vertical distributions of the MSA:nss $SO_4^=$ ratio as derived solely from the oceanic DMS source of the two compounds.

similar in pattern to Figure 6). Observation and modeling of the Antarctic boundary layer (Palmer peninsula) by *Davis et al.* [1998] led these authors to suggest the existence of a ''buffer layer'' above the boundary layer. These authors suggest that large boundary layer aerosol loadings followed by dry deposition to the Earth's surface rapidly scavenged or removed oxidized sulphur species from the lower atmosphere. Thus, lifetimes for most species such as MSA and H_2SO_4 in this layer are typically short (2 hours or less). They further suggest that the reduced UV levels (and hence the photochemically produced DMS oxidant OH) in the boundary layer lead to an extended DMS lifetime (up to 9 days) in this region. Vertical transport brings this DMS into the buffer layer, where in the presence of elevated OH, it is converted into its typical products, among which are MSA and H_2SO_4. Reduced dry deposition from the buffer layer to the Earth's surface results in elevated concentrations of these oxidation products at upper levels relative to the boundary layer. Although the phenomenon of a buffer layer is not consciously included in our model, TM3 has reproduced its existence in the Antarctic atmosphere, with the MSA:nss $SO_4^=$ ratios being highest just above the boundary layer concentrations, with the exception of the summer months (not shown, but similar in pattern to Figure 6).

[33] Overall, TM3 model performance in simulating the atmospheric MSA:nss $SO_4^=$ ratio derived from all sources is fair (i.e., a general overestimation of 23%; degrees of freedom = 90) in all areas of the globe where actual measure-

ments of the ratio have been made (i.e., the Atlantic Ocean, Pacific Ocean, Indian Ocean, Southern Ocean, Antarctica, and the Arctic).

3.2. Ratios Considering Only the Oceanic DMS Sulphur Source

[34] Here we present results on the MSA:nss $SO_4^=$ ratio as it results solely from the marine DMS sulphur source (i.e., excluding the contribution from all other sources). From a measurement and data correction point of view, such information could help in estimating the fraction of MSA or nss $SO_4^=$ in ''total'' ratios that may be due to oceanic DMS only. It is also useful in determining the relative yields of MSA and nss $SO_4^=$ from the atmospheric oxidation of ocean-leaving DMS, at various locations during different periods. Current information used in the TM3 model on the ratio of DMS oxidation products in the atmosphere (MSA versus the nss $SO_4^=$ precursor gas: SO_2) under different environmental conditions is uncertain. By comparing model-determined ratios of the yields of MSA and nss $SO_4^=$ to field observations, the level of uncertainty in the model parameterizations on this issue can be estimated.

[35] At the same time, it should be noted that while MSA is a direct product of atmospheric DMS oxidation, nss $SO_4^=$ is not (i.e., it is derived from SO_2, which is a direct product of DMS oxidation). As such, a lag in the timing of the peak concentrations of MSA and nss $SO_4^=$ originating from a specific DMS-oxidation event can be expected. This reduces the accuracy of the MSA:nss $SO_4^=$ ratio derived from only the oceanic DMS source, in providing information about the relative yields of these products from a specific DMS-oxidation event. Introducing a correction factor for the time lag or accumulation effects in the MSA and nss $SO_4^=$ concentrations used to derive the ratios might strengthen the usefulness of the ratio and its comparability to laboratory kinetic experiments.

[36] Model results on the MSA:nss $SO_4^=$ ratio derived from the oceanic DMS source alone are compared to measurements, where available in Table 2, and discussed later in the text. Figure 7 shows the horizontal surface distribution of MSA:nss $SO_4^=$ ratios as derived solely from the oceanic DMS source of the two compounds. It is evident that when the contribution of all other sulphur sources (especially the anthropogenic source) is not included in the ratio calculations, the signals of MSA and nss $SO_4^=$ derived from oceanic DMS in the middle and high latitudes of the Northern Hemisphere are highlighted. These signals are otherwise masked in maps showing the spatial distribution of ratios which consider all sulphur sources (see Figures 4 and 5). Elsewhere on the globe (specifically in the Southern Hemisphere), differences between the ratios considering all sulphur sources (Figures 4 and 5) and those considering the contribution of only the oceanic DMS sulphur source (Figure 7) are minimal. In the Southern Hemisphere, this may be attributed to a reduced level of industrialization (therefore, a weak industrial sulphur source).

[37] During the Atmosphere/Ocean Chemistry Experiment (AEROCE) at Bermuda, Barbados, Tenerife, and Mace Head in Ireland, *Savoie et al.* [2002] used antimony and aerosol nitrate as tracers for anthropogenic input, in order to independently estimate the contribution of marine DMS to total MSA:nss $SO_4^=$ ratios being observed. Their results are compared to model results in Table 2. TM3 seems to overestimate the ratio at Barbados, Bermuda, and Tenerife by a factor of 5. The ratio predicted for summer at Mace Head is in fair agreement with the observed, however, in winter the ratio is overestimated by a factor of 10. *McArdle et al.* [1998] similarly conducted isotopic analyses for aerosol samples collected at Mace Head and observed the MSA to biogenic sulphate ratio to be $\sim$0.67 during June and July. For this location, TM3 predicts a ratio of about half the observed value (Table 2).

[38] The TM3 model overpredicts the MSA:nss $SO_4^=$ in the Antarctic atmosphere (a factor of 3 for Neumayer station, 4 for Mawson, and a factor of 5 for Dumont D'Urville at the annual scale). As was mentioned earlier, the Antarctic coastline exhibits sharp gradients in the MSA:nss $SO_4^=$ ratio and so even a slight displacement of specific isopleths in the model year versus the measurement years can lead to a mismatch between the simulated and observed ratio for a given coastal Antarctic station. In spite of such overprediction at some locations, seasonal trends in the MSA:nss $SO_4^=$ ratio is well emulated by the model at most stations (see Figure 3).

[39] Overall, the model-observations comparisons for the MSA:nss $SO_4^=$ ratio derived solely from oceanic DMS are not quite satisfactory (i.e., a general overestimation of a factor of 3; degrees of freedom = 50). Inadequacies in the methodologies used to deduce the MSA to biogenic sulphate fraction in observations, as well as shortcomings in the TM3 parameterizations on the relative yields of DMS oxidation products, may all lead to a mismatch between modeled and observed values. In addition, the measurement locations are still too few in number to make conclusive remarks about the ability of TM3 to simulate the yield of MSA, relative to nss $SO_4^=$, from the oxidation of marine DMS. Improvement of model parameterizations and continued spatially comprehensive measurements are necessary for better comparisons.

[40] Zonal vertical distributions of MSA:nss $SO_4^=$ ratios derived solely from the oceanic DMS source of the two compounds (Figure 6) reveal that in the middle and high latitudes, the yield of MSA relative to nss $SO_4^=$ within the model is highest above the boundary layer. This may be attributed to enhanced removal through wet and dry deposition in the boundary layer. As was mentioned earlier, MSA has typically been found to exist on larger particles than nss $SO_4^=$, and as such, it may be deposited at a faster rate than nss $SO_4^=$ within the boundary layer, where precipitation occurs, surface roughness is highest, and where atmospheric turbulence is greatest [*König-Langlo et al.*, 1998; *Kottmeier and Fay*, 1998]. *Davis et al.* [1999] have also suggested that the heterogeneous processes involving the formation of MSA and nss $SO_4^=$ may have different temperature dependencies, and quite possibly are influenced to different degrees by the availability of oxidizing agents on aerosol surfaces or levels of oxidants in the aqueous phase. This too may affect the observed MSA:nss $SO_4^=$ ratio.

4. Summary and Conclusions

[41] MSA is formed exclusively from DMS, while the climate-relevant nss $SO_4^=$ has a variety of sources which

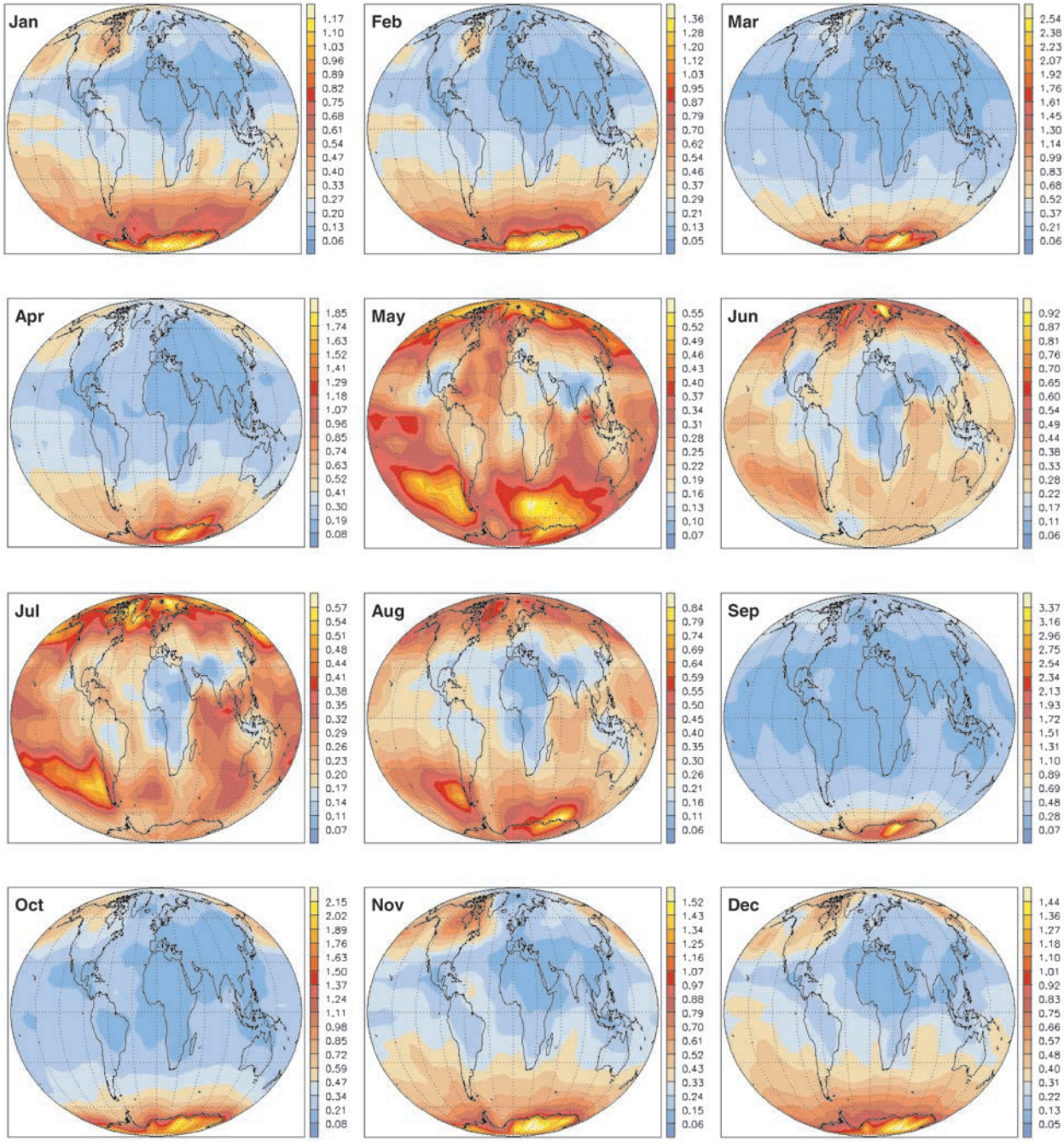

Figure 7. Global monthly mean surface (~1009 hPa) distribution of TM3-modeled MSA:nss $SO_4^=$ ratio as derived solely from the oceanic DMS source of the two compounds.

include atmospheric DMS oxidation and volcanic and anthropogenic sulphur emissions. As such, the methanesulphonate to non sea salt sulphate ratio provides an indication of the relative contributions of DMS and anthropogenic sources to total sulphate levels. A high ratio suggests that a considerable fraction of the total nss $SO_4^=$ being observed is derived from the atmospheric oxidation of DMS, while a low ratio implies that the contribution of DMS to the total nss $SO_4^=$ being observed is low.

[42] Interpretation of measurements of the MSA:nss $SO_4^=$ ratio in ice cores and in the atmosphere has led to the consensus that DMS is a considerable source of sulphur in the marine atmosphere (e.g., *Legrand* [1995] and references within Table 1). However, due to the sparsity of the measurements, a comprehensive picture of the globe-wide spatial and temporal distribution of the ratio has not been available. In this study, we have made use of a 3-D global chemical transport model to complement measurements of

the MSA:nss $SO_4^=$ ratio with the aim of providing such a complete picture.

[43] On the basis of model-observation comparisons, it is observed that the MSA:nss $SO_4^=$ ratio (resulting from both all sulphur sources and the ocean DMS source alone) is highest around the polar regions and lowest within the tropics. This is attributed to the fact that MSA production is most effective under low temperatures. We also propose that on a seasonal scale, temperature and the extent of biological activity are not the only controlling mechanisms of atmospheric MSA concentrations. Light conditions are also important. Inexistent photochemical production of hydroxyl radicals during the dark winter months at high latitudes limits MSA production through the reaction of DMS and these radicals.

[44] On a hemispheric scale, the highest ratios occur in the Southern Hemisphere, throughout the year, despite multiyear satellite-deduced primary production showing great concentration of marine phytoplankton at middle to high latitudes in the opposite (Northern) Hemisphere. This is attributed to the fact that the atmospheric DMS burden is also highest in this region [*Gondwe et al.*, 2003a, 2003b]. Anthropogenic sulphur emissions in the highly industrialized Northern Hemisphere lead to a lower MSA:nss $SO_4^=$ ratio in the Northern Hemisphere.

[45] Results from the TM3 model provide a first step toward improving our understanding of how the ratio can vary over time and space, assuming that the parameterizations in the model are correct. Overall, TM3 model performance in simulating the atmospheric MSA:nss $SO_4^=$ ratio derived from all sources (section 3.1) is fair (i.e., a general overestimation of 23%; degrees of freedom = 90) in all areas where actual measurements of the ratio have been made (i.e., the Atlantic Ocean, Pacific Ocean, Indian Ocean, Southern Ocean, Antarctica, and the Arctic).

[46] On the other hand, the model-observation comparisons for the MSA:nss $SO_4^=$ ratio derived solely from the oceanic DMS source (section 3.2) are not quite satisfactory (an overall overestimation of a factor of 3; degrees of freedom = 50). Shortcomings in the TM3 parameterizations on the relative yields of DMS oxidation products, as well as inadequacies in the methodologies used to deduce the MSA to biogenic sulphate fraction in observations, may all lead to a mismatch between modeled and observed values. In addition, the measurement locations are still too few in number to make conclusive remarks about the ability of TM3 to simulate the yield of MSA, relative to nss $SO_4^=$, from the oxidation of marine DMS. Improvement of model parameterizations and continued spatially comprehensive measurements are necessary for better comparisons.

[47] Specifically, current information on in-water and atmospheric DMS (photo)chemistry and kinetics is limited and based on a few pioneering works [e.g., *Hynes et al.*, 1986; *Martin et al.*, 1987; *Barnes et al.*, 1987, 1989a, 1989b; *Hynes and Wine*, 1989; *Adewuyi*, 1989; *Hearn et al.*, 1990; *Atkinson et al.*, 1992; *Barone et al.*, 1995; *Arsene et al.*, 2001]. More work to improve on this information is vital. Furthermore, not only should measurements of DMS and its oxidation products in water, the atmosphere, and precipitation be continued, but they should also be extended to regions of the globe that are not typical study sites or locations of extensive algal blooms (e.g., the oligotrophic oceans). Currently measurements are often made in areas where algal blooms are frequent, intense, and extensive or where sampling stations already exist. Such within-bloom measurement is necessary for in-water studies of environmental-related aspects of DMS, while existing sampling stations offer the opportunity to continue time series measurements. However, it is now clear that in the atmosphere high concentrations of DMS oxidation products are not necessarily confined to regions of high primary production [e.g., *Gondwe et al.*, 2003a, 2003b], partly due to the dynamic nature of the atmospheric medium (i.e., transport of chemical elements from region to region and (non)-accumulation effects due to specific prevailing atmospheric circulation patterns).

[48] The existence of products of DMS oxidation (other than MSA and SO_2) such as DMSO (dimethylsulphoxide) and $DMSO_2$ (dimethylsulphone) has also been confirmed through laboratory experiments [e.g., *Yin et al.*, 1990a, 1990b] and measurements [e.g., *Harvey and Lang*, 1986; *Hatton et al.*, 1996; *Davis et al.*, 1998; *Chen et al.*, 2000; *Sciare et al.*, 2000a] alike. However, detailed information on their yield relative to other oxidation products in the atmosphere is limited and needs to be improved. At present, only MSA and SO_2 are considered as the only direct products of DMS oxidation in the TM3 model. Inclusion of other oxidation products would change the yield of MSA and SO_2 from DMS oxidation in the model and perhaps result in better agreement between model results and in situ measurements.

[49] The estimation of the sea-to-air flux of gases also has some uncertainties. Efforts such as those of *Hintsa et al.* [2004] and *Zemmelink et al.* [2004] in using new methodologies in determining the sea-to-air flux of DMS make an important contribution toward better parameterization of the sea-to-air flux of DMS in models. Such efforts too need to be expanded to cover a broader region of the globe.

[50] **Acknowledgments.** F. Dentener (Joint Research Centre, Italy) and A. Jeuken (Institute for Inland Water Management and Wastewater Treatment, Netherlands) are gratefully acknowledged for preparing and supplying the TM3 source code. Model output was analyzed using *HipHop* (thanks to D. Brunner, Institute for Atmospheric and Climate Science, Switzerland). This project has been conducted within the framework of the Surface Ocean Lower Atmosphere Study (SOLAS) and has been financially supported by the Netherlands Space Research Organisation (SRON Project EO-033). A reviewer of a previous paper by the authors is gratefully acknowledged for bringing us on the idea for this article. We also thank an anonymous reviewer for very constructive comments on the manuscript of this paper.

References

Adewuyi, Y. G. (1989), Oxidation of biogenic sulphur compounds in aqueous media, in *Biogenic Sulphur in the Environment*, edited by E. S. Saltzman and W. J. Cooper, pp. 529–559, Am. Chem. Soc., Washington D. C.

Albrecht, B. A. (1989), Aerosols, cloud microphysics, and fractional cloudiness, *Science*, *245*, 1227–1230.

Andreae, M. O., W. Elbert, and S. J. de Mora (1995), Biogenic sulphur emissions and aerosols over the tropical south Atlantic: 3. Atmospheric dimethylsulphide, aerosols, and cloud condensation nuclei, *J. Geophys. Res.*, *100*, 11,335–11,356.

Andres, R. J., and A. D. Kasgnoc (1998), A time-averaged inventory of subaerial volcanic sulphur emissions, *J. Geophys. Res.*, *103*, 25,251–25,261.

Arsene, C., I. Barnes, K. H. Becker, and R. Mocanu (2001), FT-IR product study on the photo-oxidation of dimethylsulphide in the presence of NO_x: Temperature dependence, *Atmos. Environ.*, *35*, 3769–3780.

Atkinson, R., D. L. Baulch, R. A. Cox, R. F. Hampson Jr., J. A. Kerr, and J. Troe (1992), Evaluated kinetic and photochemical data for atmospheric chemistry: Supplement IV, *Atmos. Environ., Part A*, *26*, 1187–1230.

Ayers, G. P., J. P. Ivey, and H. S. Goodman (1986), Sulphate and methanesulphonate in the maritime aerosol at Cape Grim, Tasmania, *J. Atmos. Chem.*, *4*, 173–185.

Ayers, G. P., J. P. Ivey, and R. W. Gillett (1991), Coherence between seasonal cycles of dimethylsulphide, methanesulphonate and sulphate in marine air, *Nature*, *349*, 404–406.

Ayers, G. P., J. M. Cainey, H. Granek, and C. Leck (1996), Dimethylsulphide oxidation and the ratio of methanesulphonate to non sea-salt sulphate in the marine aerosol, *J. Atmos. Chem.*, *25*, 307–325.

Barnes, I., K. H. Becker, P. Carlier, and G. Mouvier (1987), FTIR study of the $DMS/NO_2/I_2/N_2$ photolysis system: The reaction of IO radicals with DMS, *Int. J. Chem. Kinet.*, *19*, 489–501.

Barnes, I., K. H. Becker, D. Martin, P. Carlier, G. Mouvier, J. L. Jourdain, G. Leverdet, and G. Le Bras (1989a), Impact of halogen oxides on dimethylsulphide oxidation in the marine atmosphere, in *Biogenic Sulphur in the Environment*, edited by E. S. Saltzman and W. J. Cooper, pp. 464–475, Am. Chem. Soc., Washington, D. C.

Barnes, I., V. Bastian, K. H. Becker, and D. Martin (1989b), Fourier transform IR studies of the reactions of dimethylsulphoxide with OH, NO_3 and Cl radicals, in *Biogenic Sulphur in the Environment*, edited by E. S. Saltzman and W. J. Cooper, pp. 476–488, Am. Chem. Soc., Washington, D. C.

Barone, S. B., A. A. Turnipseed, and A. R. Ravishankara (1995), Role of adducts in the atmospheric oxidation of dimethylsulphide, *Faraday Discuss.*, *100*, 39–54.

Bates, T. S., J. E. Johnson, P. K. Quinn, P. D. Goldan, W. C. Kuster, D. C. Covert, and C. J. Hahn (1990), The biogeochemical sulphur cycle in the marine boundary layer over the northeast Pacific Ocean, *J. Atmos. Chem.*, *10*, 59–81.

Bates, T. S., B. K. Lamb, A. Guenther, J. Dignon, and R. E. Stoiber (1992), Sulphur emissions to the atmosphere from natural sources, *J. Atmos. Chem.*, *14*, 315–337.

Bergin, M. H., J. L. Jaffrezo, C. I. Davidson, R. Caldow, and J. Dibb (1994), Fluxes of chemical species to the Greenland ice sheet at Summit by fog and dry deposition, *Geochim. Cosmochim. Acta*, *58*, 3207–3215.

Bergin, M. H., J. L. Jaffrezo, C. I. Davidson, J. E. Dibb, S. N. Pandis, R. Hillamo, W. Maenhaut, H. D. Kuhns, and T. Makela (1995), The contributions of snow, fog, and dry deposition to the summer flux of anions and cations at Summit, Greenland, *J. Geophys. Res.*, *100*, 16,275–16,288.

Berresheim, H. (1987), Biogenic sulphur emissions from the Subantarctic and Antarctic Oceans, *J. Geophys. Res.*, *92*, 13,245–13,262.

Berresheim, H., M. O. Andreae, G. P. Ayers, R. W. Gillett, J. T. Merrill, V. J. Davis, and W. L. Chameides (1990), Airborne measurements of dimethylsulphide, sulphur dioxide and aerosol ions over the southern ocean south of Australia, *J. Atmos. Chem.*, *10*, 341–370.

Berresheim, H., M. O. Andreae, R. L. Iverson, and S. M. Li (1991), Seasonal variations of dimethylsulphide emissions and atmospheric sulphur and nitrogen species over the western North Atlantic Ocean, *Tellus, Ser. B*, *43*, 353–372.

Berresheim, H., J. W. Huey, R. P. Thorn, F. L. Eisele, D. J. Tanner, and A. Jefferson (1998), Measurements of dimethylsulphide, dimethylsulphoxide, dimethylsulphone and aerosol ions at Palmer Station, Antarctica, *J. Geophys. Res.*, *103*, 1629–1637.

Boucher, O., and U. Lohmann (1995), The Sulfate-CCN-Cloud albedo effect: A sensitivity study with two general circulation models, *Tellus, Ser. B*, *47*, 281–300.

Campolongo, F., A. Saltelli, N. R. Jensen, J. Wilson, and J. Hjorth (1999), The role of multiphase chemistry in the oxidation of dimethylsulphide (DMS): A latitude dependent analysis, *J. Atmos. Chem.*, *32*, 327–356.

Charlson, R. J., J. E. Lovelock, M. O. Andreae, and S. G. Warren (1987), Oceanic plankton, atmospheric sulphur, cloud albedo and climate, *Nature*, *326*, 655–661.

Chen, G., D. D. Davis, P. Kasibhatla, A. R. Bandy, D. C. Thornton, B. J. Huebert, A. D. Clarke, and B. W. Blomquist (2000), A study of DMS oxidation in the tropics: Comparison of Christmas Island field observations of DMS, SO_2 and DMSO with model simulations, *J. Atmos. Chem.*, *37*, 137–160.

Davidson, C. I., S. Santhanam, R. C. Fortmann, and M. P. Olson (1985), Atmospheric transport and deposition of trace elements onto the Greenland ice sheet, *Atmos. Environ.*, *19*, 2065–2081.

Davidson, C. I., et al. (1993a), Chemical constituents in the air and snow at Dye 3, Greenland: 1. Seasonal variations, *Atmos. Environ., Part A*, *27*, 2709–2722.

Davidson, C. I., J. L. Jaffrezo, M. J. Small, P. W. Summers, M. P. Olson, and R. D. Borys (1993b), Trajectory analysis of source regions influencing the South Greenland ice sheet during the Dye 3 gas and aerosol sampling program, *Atmos. Environ., Part A*, *27*, 2739–2749.

Davis, D., G. Chen, P. Kasibhatla, A. Jefferson, D. Tanner, F. Eisele, D. Lenschow, W. Neff, and H. Berresheim (1998), DMS oxidation in the Antarctic marine boundary layer: Comparison of model simulations and field observations of DMS, DMSO, $DMSO_2$, H_2SO_4(g), MSA(g), and MSA(p), *J. Geophys. Res.*, *103*, 1657–1678.

Davis, D., et al. (1999), Dimethylsulphide oxidation in the equatorial Pacific: Comparison of model simulations with field observations for DMS, SO_2, H_2SO_4(g), MSA(g), MS, and NSS, *J. Geophys. Res.*, *104*, 5765–5784.

Davison, B., and C. N. Hewitt (1992), Natural sulphur species from the North Atlantic and their contribution to the United Kingdom sulphur budget, *J. Geophys. Res.*, *97*, 2475–2488.

Delmas, R. J., P. Wagnon, K. Goto-Azuma, K. Kamiyama, and O. Watanabe (2003), Evidence for the loss of snow-deposited MSA to the interstitial gaseous phase in central Antarctic firn, *Tellus, Part B.*, *55*, 71–79.

Dentener, F., J. Feichter, and A. Jeuken (1999), Simulation of the transport of Rn^{222} using on-line and off-line global models at different horizontal resolutions: A detailed comparison with measurements, *Tellus, Ser. B*, *51*, 573–602.

Dentener, F., J. Williams, and S. Metzger (2002), Aqueous phase reaction of HNO_4: The impact on tropospheric chemistry, *J. Atmos. Chem.*, *41*, 109–134.

Galloway, J. N., W. C. Keene, A. A. Pszenny, D. Whelpdale, H. Sievering, J. Merrill, and J. Boatman (1990), Sulphur in the western North Atlantic Ocean atmosphere: Results from a summer 1988 ship/aircraft experiment, *Global Biogeochem. Cycles*, *4*, 349–365.

Galloway, J. N., D. L. Savoie, W. C. Keene, and J. M. Prospero (1993), The temporal variability of scavenging ratios for nss sulphate, nitrate, methanesulphonate and sodium in the atmosphere over the North Atlantic Ocean, *Atmos. Environ.*, *27*, 235–250.

Gillett, R. W., G. P. Ayers, J. P. Ivey, and J. L. Gras (1993), Measurement of dimethylsulphide, sulphur dioxide, methane sulphonic acid and non sea salt sulphate at the Cape Grim baseline station, in *Dimethylsulphide: Oceans, Atmosphere and Climate*, edited by G. Restelli and G. Angeletti, pp. 117–128, Kluwer Acad., Norwell, Mass.

Gondwe, M., M. Krol, W. Klaassen, W. Gieskes, and H. de Baar (2003a), The contribution of ocean-leaving DMS to the global atmospheric burdens of DMS, MSA, SO_2 and nss $SO_4^=$, *Global Biogeochem. Cycles*, *17*(2), 1056, doi:10.1029/2002GB001937.

Gondwe, M., M. Krol, W. Klaassen, W. Gieskes, and H. de Baar (2003b), Correction to "The contribution of ocean-leaving DMS to the global atmospheric burdens of DMS, MSA, SO_2 and nss $SO_4^=$," *Global Biogeochem. Cycles*, *17*(4), 1106, doi:10.1029/2003GB002153.

Hansson, M. E., and E. S. Saltzman (1993), The first Greenland ice core record of methanesulphonate and sulphate over a full glacial cycle, *Geophys. Res. Lett.*, *20*, 1163–1166.

Harder, S. L., S. G. Warren, R. J. Charlson, and D. S. Covert (1996), Filtering of air through snow as a mechanism for aerosol deposition to the Antarctic ice sheet, *J. Geophys. Res.*, *101*, 18,729–18,743.

Harvey, G. R., and R. F. Lang (1986), Dimethylsulphoxide and dimethylsulphone in the marine atmosphere, *Geophys. Res., Lett.*, *13*, 49–51.

Hatton, A. D., G. Malin, S. M. Turner, and P. S. Liss (1996), DMSO: A significant compound in the biogeochemical cycle of DMS, in *Biological and Environmental Chemistry of DMSP and Related Sulphonium Compounds*, edited by R. P. Kiene et al., pp. 405–412, Plenum, New York.

Hearn, C. H., E. Turcu, and J. A. Joens (1990), The near U.V. absorption spectra of dimethylsulphide, diethylsulphide, and dimethyldisulphide, at $T = 300$ K, in *Atmos. Environ., Part A*, 1939–1944.

Hines, M. E., R. E. Pelletier, and P. M. Crill (1993), Emissions of sulphur gases from marine and freshwater wetlands of the Florida Everglades: Rates and extrapolation using remote sensing, *J. Geophys. Res.*, *98*, 8991–8999.

Hintsa, E. J., J. W. H. Dacey, W. R. McGillis, J. B. Edson, C. J. Zappa, and H. J. Zemmelink (2004), Sea-to-air fluxes from measurements of the atmospheric gradient of dimethylsulfide and comparison with simultaneous relaxed eddy accumulation measurements, *J. Geophys. Res.*, 109, C01026, doi:10.1029/2002JC001617.

Hobbs, P., and T. Mottram (2000), Significant contributions of dimethylsulphide from livestock to the atmosphere, *Atmos. Environ.*, *34*, 3649–3650.

Houweling, S., F. Dentener, and J. Lelieveld (1998), The impact of non-methane hydrocarbon compounds on tropospheric photochemistry, *J. Geophys. Res.*, *103*, 10,673–10,696.

Huebert, B. J., S. Howell, P. Laj, J. E. Johnston, T. S. Bates, P. K. Quinn, V. Yegorov, A. D. Clarke, and J. N. Porter (1993), Observations of the atmospheric sulphur cycle on SAGA 3, *J. Geophys. Res.*, *98*, 16,985–16,995.

Hynes, A. J., and P. H. Wine (1989), OH-initiated oxidation of biogenic sulphur compounds: Kinetics and mechanisms under atmospheric conditions, in *Biogenic Sulphur in the Environment*, edited by E. S. Saltzman and W. J. Cooper, pp. 424–436, Am. Chem. Soc., Washington, D. C.

Hynes, A. J., P. H. Wine, and D. H. Semmes (1986), Kinetics and mechanism of OH reactions with organic sulphides, *J. Phys. Chem.*, *90*, 4148–4156.

Intergovernmental Panel on Climate Change (IPCC) (2001), *Climate Change 2001: The Scientific Basis*, edited by J. T. Houghton et al., Cambridge Univ. Press, New York.

Ivey, J. P., D. M. Davies, V. Morgan, and G. P. Ayers (1986), Methanesulphonate in Antarctic ice, *Tellus, Ser. B*, *38*, 375–379.

Jaffrezo, J. L., C. I. Davidson, M. Legrand, and J. E. Dibb (1994), Sulphate and MSA in the air and snow on the Greenland Ice Sheet, *J. Geophys. Res.*, *99*, 1241–1253.

Jefferson, A., D. J. Tanner, F. L. Eisele, D. D. Davis, G. Chen, J. Crawford, J. W. Huey, A. L. Torres, and H. Berresheim (1998), OH photochemistry and methane sulphonic acid formation in the coastal Antarctic boundary layer, *J. Geophys. Res.*, *103*, 1647–1656.

Jeuken, A., J. P. Veefkind, F. Dentener, S. Metzger, and C. Robles Gonzalez (2001), Simulation of the aerosol optical depth over Europe for August 1997 and a comparison with observations, *J. Geophys. Res.*, *106*, 28,295–28,311.

Kettle, A. J., et al. (1999), A global database of sea surface dimethylsulphide (DMS) measurements and a procedure to predict sea surface DMS as a function of latitude, longitude and month, *Global Biogeochem. Cycles*, *13*, 399–444.

Kiene, R. P., L. J. Linn, and J. A. Bruton (2000), New important roles for DMSP in marine microbial communities, *J. Sea Res.*, *43*, 209–224.

König-Langlo, G., J. King, and P. Pettre (1998), Climatology of the three coastal Antarctic stations Dumont D'Urville, Neumayer, and Halley, *J. Geophys. Res.*, *103*, 10,935–10,946.

Kottmeier, C., and B. Fay (1998), Trajectories in the Antarctic lower troposphere, *J. Geophys. Res.*, *103*, 10,947–10,959.

Kouvarakis, G., and N. Mihalopoulos (2002), Seasonal variation of dimethylsulphide in the gas phase and of methanesulphonate and non-sea-salt sulphate in the aerosols phase in the Eastern Mediterranean atmosphere, *Atmos. Environ.*, *36*, 929–938.

Kreidenweis, S. M., J. E. Penner, F. Yin, and J. H. Seinfeld (1991), The effects of dimethylsulphide upon marine aerosol concentrations, *Atmos. Environ.*, *25*, 2501–2511.

Kreutz, K. J., P. A. Mayewski, S. I. Whitlow, and M. S. Twickler (1998), Limited migration of soluble ionic species in a Siple Dome, Antarctica, ice core, *Ann. Glaciol.*, *27*, 371–377.

Legrand, M. (1995), Sulphur-derived species in polar ice: A review, in *Ice Core Studies of Global Biogeochemical Cycles*, edited by R. J. Delmas, *NATO ASI Ser.*, vol. 130, pp. 91–119, Springer-Verlag, New York.

Legrand, M., and E. C. Pasteur (1998), Methane sulphonic acid to non-sea-salt sulphate ratio in coastal Antarctic aerosol and surface snow, *J. Geophys. Res.*, *103*, 10,991–11,006.

Legrand, M., C. Feniet-Saigne, E. S. Saltzman, C. Germain, N. I. Barkov, and V. N. Petrov (1991), Ice-core record of oceanic emissions of dimethylsulphide during the last climate cycle, *Nature*, *350*, 144–146.

Legrand, M., C. Feniet-Saigne, E. S. Saltzman, and C. Germain (1992), Spatial and temporal variations of methanesulphonic acid and non sea salt sulphate in Antarctic ice, *J. Atmos. Chem.*, *14*, 245–260.

Legrand, M., C. Hammer, M. De Angelis, J. Savarino, D. Delmas, H. Clausen, and S. J. Johnsen (1997), Sulphur-containing species (methanesulphonate and SO_4) over the last climatic cycle in the Greenland Ice Core Project (central Greenland) ice core, *J. Geophys Res.*, *102*, 26,663–26,679.

Li, S. M., and L. A. Barrie (1993), Biogenic sulphur aerosol in the Arctic troposphere: 1. Contributions to total sulphate, *J. Geophys. Res.*, *98*, 20,613–20,622.

Li, S. M., L. A. Barrie, R. W. Talbot, R. C. Harriss, C. I. Davidson, and J. L. Jaffrezo (1993), Seasonal and geographic variations of methanesulphonic acid in the Arctic troposphere, *Atmos. Environ.*, *27*, 3011–3024.

Liss, P. S., and L. Merlivat (1986), Air-sea gas exchange rates: Introduction and synthesis, in *The Role of Air-Sea Exchange in Geochemical Cycling*, edited by P. Buat-Menard, pp. 113–127, D. Reidel, Norwell, Mass.

Martin, D., J. L. Jourdain, G. Laverdet, and G. Le Bras (1987), Kinetic study of the reaction of IO with CH_3SCH_3, *Int. J. Chem. Kinet.*, *19*, 503–512.

Mauldin, R. L., D. J. Tanner, J. A. Heath, B. J. Huebert, and F. L. Eisele (1999), Observations of H_2SO_4 and MSA during PEM-Tropics-A, *J. Geophys. Res.*, *104*, 5801–5816.

McArdle, N. C., and P. S. Liss (1995), Isotopes and atmospheric sulphur, *Atmos. Environ.*, *29*, 2553–2556.

McArdle, N., P. Liss, and P. Dennis (1998), An isotopic study of atmospheric sulphur at three sites in Wales and at Mace Head, Eire, *J. Geophys. Res.*, *103*, 31,079–31,094.

Minikin, A., D. Wagenbach, W. Graf, and J. Kipfstuhl (1994), Spatial and seasonal variations of the snow chemistry at central Filchner-Ronne Ice Shelf, Antarctica, *Ann. Glaciol.*, *20*, 283–290.

Minikin, A., M. Legrand, J. Hall, D. Wagenbach, C. Kleefeld, E. Wolff, E. C. Pasteur, and F. Ducroz (1998), Sulphur-containing species (sulphate and methanesulphonate) in coastal Antarctic aerosol and precipitation, *J. Geophys. Res.*, *103*, 10,975–10,990.

Mulvaney, R., and E. Wolff (1994), Spatial variability of the major chemistry of the Antarctic ice sheet, *Ann. Glaciol.*, *20*, 440–447.

Mulvaney, R., E. C. Pasteur, D. A. Peel, E. S. Saltzman, and P.-Y. Whung (1992), The ratio of MSA to non-sea-salt sulphate in Antarctic Peninsula ice cores, *Tellus*, *44*, 295–303.

O'Dowd, C. O., J. A. Lowe, M. H. Smith, B. Davison, C. N. Hewitt, and R. M. Harrison (1997), Biogenic sulphur emissions and inferred non-sea-salt-sulphate cloud condensation nuclei in and around Antarctica, *J. Geophys. Res.*, *102*, 12,839–12,854.

Olivier, J. G. J., and J. J. M. Berdowski (2001), Global emission sources and sinks, in *The Climate System*, edited by J. Berdowski et al., pp. 33–77, Swets and Zeitlinger, Lisse, Netherlands.

Parish, T. R., and D. H. Bromwich (1991), Continental-scale simulation of the Antarctic katabatic wind regime, *J. Clim.*, *4*, 135–146.

Pasteur, E. C., and R. Mulvaney (1999), Laboratory study of the migration of methane sulphonate in firn, *J. Glaciol.*, *45*, 214–218.

Pasteur, E. C., and R. Mulvaney (2000), Migration of methane sulphonate in Antarctic firn air and ice, *J. Geophys. Res.*, *105*, 11,525–11,534.

Pasteur, E. C., R. Mulvaney, D. A. Peel, E. S. Saltzman, and P. Y. Whung (1995), A 340 year record of biogenic sulphur from the Weddell sea area, Antarctica, *Ann. Glaciol.*, *21*, 169–174.

Prospero, J. M., D. L. Savoie, E. S. Saltzman, and R. Larsen (1991), Impact of oceanic sources of biogenic sulphur on sulphate aerosol concentrations at Mawson, Antarctica, *Nature*, *350*, 221–223.

Prospero, J. M., D. L. Savoie, R. Arimoto, H. Olafsson, and H. Hjartarson (1995), Sources of aerosol nitrate and non-sea-salt sulphate in the Iceland region, *Sci. Total Environ.*, *160/161*, 181–191.

Pszenny, A. A. P., A. J. Castelle, and J. N. Galloway (1989), A study of the sulphur cycle in the Antarctic marine boundary layer, *J. Geophys. Res.*, *94*, 9818–9830.

Pszenny, A. A. P., G. R. Harvey, C. J. Brown, R. F. Lang, W. C. Keene, J. N. Galloway, and J. T. Merrill (1990), Measurements of dimethylsulphide oxidation products in the summertime North Atlantic marine boundary layer, *Global Biogeochem. Cycles*, *4*, 367–379.

Saigne, C., and M. Legrand (1987), Measurements of methanesulphonic acid in Antarctic ice, *Nature*, *330*, 240–242.

Saltzman, E. S., D. L. Savoie, R. G. Zika, and J. M. Prospero (1983), Methane sulfonic acid in the marine atmosphere, *J. Geophys. Res.*, *88*, 10,897–10,902.

Saltzman, E. S., D. L. Savoie, J. M. Prospero, and R. G. Zika (1985), Atmospheric methanesulphonic acid and non-sea salt sulphate at Fanning and American Samoa, *Geophys. Res. Lett.*, *12*, 437–440.

Saltzman, E. S., D. L. Savoie, J. M. Prospero, and R. G. Zika (1986), Methanesulphonic acid and non-sea-salt sulphate in Pacific air: Regional and seasonal variations, *J. Atmos. Chem.*, *4*, 227–240.

Saltzman, E. S., P.-Y. Whung, and P. A. Mayewski (1997), Methanesulphonate in the Greenland Ice Sheet Project 2 Ice Core, *J. Geophys. Res.*, *102*, 26,649–26,657.

Savoie, D. L., and J. M. Prospero (1989), Comparison of oceanic and continental sources of non-sea salt sulphate over the Pacific Ocean, *Nature*, *339*, 685–687.

Savoie, D. L., J. M. Prospero, and E. S. Saltzman (1989), Nitrate, non-sea-salt sulphate and methanesulphonate over the Pacific Ocean, in *Chemical Oceanography*, vol. 10, edited by J. P. Riley et al., pp. 219–250, Academic, San Diego, Calif.

Savoie, D. L., J. M. Prospero, R. J. Larsen, and E. S. Saltzman (1992), Nitrogen and sulphur species in aerosols at Mawson, Antarctica, and their relationship to natural radionuclides, *J. Atmos. Chem.*, *14*, 181–204.

Savoie, D. L., J. M. Prospero, R. J. Larsen, F. Huang, M. A. Izaguirre, T. Huang, T. H. Snowdon, L. Custals, and C. G. Sanderson (1993),

Nitrogen and sulphur species in Antarctic Aerosols at Mawson, Palmer Station, and Marsh (King George Island), *J. Atmos. Chem.*, *17*, 95–122.

Savoie, D. L., J. M. Prospero, R. Arimoto, and R. A. Duce (1994), Non-sea-salt sulphate and methanesulphonate at American Samoa, *J. Geophys. Res.*, *99*, 3587–3596.

Savoie, D. L., R. Arimoto, W. C. Keene, J. M. Prospero, R. A. Duce, and J. N. Galloway (2002), Marine biogenic and anthropogenic contributions to non-sea-salt sulphate in the marine boundary layer over the North Atlantic Ocean, *J. Geophys. Res.*, *107*(D18), 4356, doi:10.1029/2001JD000970.

Sciare, J., E. Baboukas, M. Kanakidou, U. Krischke, S. Belviso, H. Bardouki, and N. Mihalopoulos (2000a), Spatial and temporal variability of atmospheric sulphur-containing gases and particles during the Albatross campaign, *J. Geophys. Res.*, *105*, 14,433–14,448.

Sciare, J., N. Mihalopoulos, and F. J. Dentener (2000b), Interannual variability of atmospheric dimethylsulphide in the southern Indian Ocean, *J. Geophys. Res.*, *105*, 26,369–26,377.

Spiro, P. A., D. J. Jacob, and J. A. Logan (1992), Global inventory of sulphur emissions with $1° \times 1°$ resolution, *J. Geophys. Res.*, *97*, 6023–6036.

Turekian, V. C., S. A. Macko, and W. C. Keene (2001), Application of stable sulphur isotopes to differentiate sources of size-resolved particulate sulphate in polluted marine air at Bermuda during spring, *Geophys. Res. Lett.*, *28*, 1491–1494.

Wagnon, P., R. J. Delmas, and M. Legrand (1999), Loss of volatile acid species from upper firn layers at Vostok, Antarctica, *J. Geophys. Res.*, *104*, 3423–3431.

Whung, P.-Y., E. S. Saltzman, M. J. Spencer, P. A. Mayewski, and N. Gundestrup (1994), Two-hundred-year record of biogenic sulphur in a south Greenland ice core (20D), *J. Geophys. Res.*, *99*, 1147–1156.

Wolff, E. W., J. S. Hall, R. Mulvaney, E. C. Pasteur, D. Wagenbach, and M. Legrand (1998), Relationship between chemistry of air, fresh snow and firn cores for aerosol species in coastal Antarctica, *J. Geophys. Res.*, *103*, 11,057–11,070.

Wylie, D. J., and S. J. de Mora (1996), Atmospheric dimethylsulphide and sulphur species in aerosol and rainwater at a coastal site in New Zealand, *J. Geophys. Res.*, *101*, 21,041–21,049.

Wylie, D. J., M. J. Harvey, S. J. de Mora, I. S. Boyd, and J. B. Liley (1993), Dimethylsulphide and aerosol measurements at Ross Island, Antarctica, in *Dimethylsulphide: Oceans, Atmosphere and Climate*, edited by G. Restelli and G. Angeletti, pp. 85–94, Kluwer Acad., Norwell, Mass.

Yin, F., D. Grosjean, and J. H. Seinfeld (1990a), Photooxidation of dimethylsulphide and dimethyldisulphide: I. Mechanism development, *J. Atmos. Chem.*, *11*, 309–364.

Yin, F., D. Grosjean, R. C. Flagan, and J. H. Seinfeld (1990b), Photooxidation of dimethylsulphide and dimethyldisulphide: II. Mechanism evaluation, *J. Atmos. Chem.*, *11*, 365–399.

Zemmelink, H. J., W. W. C. Gieskes, W. Klaassen, W. J. Beukema, H. W. de Groot, H. J. W. de Baar, E. J. Hintsa, W. R. McGillis, and J. W. H. Dacey (2004), Relaxed eddy accumulation measurements of the sea-to-air transfer of dimethylsulfide over the northeastern Pacific, *J. Geophys. Res.*, *109*, C01025, doi:10.1029/2002JC001616.

H. de Baar, Royal Netherlands Institute for Sea Research (KNIOZ), P.O. Box 59, NL-1790 AB Texel, Netherlands. (debaar@nioz.nl)

W. Gieskes, M. Gondwe, and W. Klaassen, Marine Biology Department, University of Groningen, Kerklaan 30, NL-9751 NN Haren, Netherlands. (w.w.c.gieskes@biol.rug.nl; p.m.van.himbergen@biol.rug.nl; w.klaassen@biol.rug.nl)

M. Krol, Institute for Marine and Atmospheric Research (IMAU), University of Utrecht, Princetonplein 5, NL-3584 CC Utrecht, Netherlands. (m.krol@phys.uu.nl)